Taylor & Francis
Taylor & Francis Group

Expert Opinion on Therapeutic Patents

ISSN: (Print) (Online) Journal homepage: https://www.tandfonline.com/loi/ietp20

Inhibitors of prostate-specific membrane antigen in the diagnosis and therapy of metastatic prostate cancer – a review of patent literature

Hyunsoo Ha, Hongmok Kwon, Taehyeong Lim, Jaebong Jang, Song-Kyu Park & Youngjoo Byun

To cite this article: Hyunsoo Ha, Hongmok Kwon, Taehyeong Lim, Jaebong Jang, Song-Kyu Park & Youngjoo Byun (2021): Inhibitors of prostate-specific membrane antigen in the diagnosis and therapy of metastatic prostate cancer – a review of patent literature, Expert Opinion on Therapeutic Patents, DOI: 10.1080/13543776.2021.1878145

To link to this article: https://doi.org/10.1080/13543776.2021.1878145

EXPERT OPINION ON THERAPEUTIC PATENTS
https://doi.org/10.1080/13543776.2021.1878145

Taylor & Francis
Taylor & Francis Group

REVIEW

Inhibitors of prostate-specific membrane antigen in the diagnosis and therapy of metastatic prostate cancer – a review of patent literature

Hyunsoo Ha [*], Hongmok Kwon [*], Taehyeong Lim, Jaebong Jang, Song-Kyu Park and Youngjoo Byun

Department of Pharmacy, College of Pharmacy, Korea University, 2511 Sejong-ro, Sejong 30019, South Korea

ABSTRACT

Introduction: Prostate-specific membrane antigen (PSMA), also known as glutamate carboxypeptidase II, is a potential target protein for imaging and treatment of patients with prostate cancer because of its overexpression during metastasis. Various PSMA-targeted imaging and therapeutic probes have been designed and synthesized based on the Lys-urea-Glu motif. Structural modifications have been made exclusively in the linker region, while maintaining the Lys-urea-Glu structure that interacts with S1 and S1′ pockets.

Area Covered: This review includes WIPO-listed patents (from January 2017 to June 2020) reporting PSMA-targeted probes based on the Lys-urea-Glu or Glu-urea-Glu structure.

Expert opinion: : PSMA-targeted imaging agents labeled with radionuclides such as fluorine-18, copper-64, gallium-68, and technetium-99m have been successfully translated into clinical phase for the early diagnosis of metastatic prostate cancer. Recently, PSMA-targeted therapeutic agents labeled with iodine-131, lutetium-177, astatine-211, and lead-212 have also been developed with notable progress. Most PSMA-targeted agents are based on the Lys-urea-Glu or Glu-urea-Glu structure, demonstrate strong PSMA-binding affinity in nanomolar range, and achieve diverse structural modifications in the non-pharmacophore pocket. By exploiting the S1 accessory pocket or the tunnel region of the PSMA active site, the *in vivo* efficacy and pharmacokinetic profiles of the PMSA-targeted agents can be effectively modulated.

ARTICLE HISTORY
Received 14 October 2020
Accepted 15 January 2021

KEYWORDS
Prostate-specific membrane antigen (PSMA); metastatic prostate cancer; imaging probes; radionuclides; Lys-urea-Glu

1. Introduction

1.1. Prostate cancer

The prostate is a walnut-shaped organ that surrounds the urethra and is located below the bladder. It is an exocrine gland that plays an important role in the male reproductive system. Prostate cancer (PCa) is the most common type of cancer and the second leading cause of cancer death in men. According to the American Cancer Society, the number of patients newly diagnosed with PCa in 2020 is estimated to be 191,930, and the number of deaths due to PCa is estimated at 33,330 [1]. Although the 5-year survival rate for localized PCa is 97.8%, that for metastatic PCa is only 30.2% [2]. In general, PCa metastases invade organs such as lymph nodes, bones, liver, and lungs [3]. Therefore, the early and accurate diagnosis of metastatic PCa is urgently needed.

Currently, PCa is diagnosed in the clinic by measuring blood levels of prostate-specific antigen (PSA) followed by a digital rectal examination (DRE) performed by a specialist. PSA is a secreted glycoprotein, and its levels increase in the presence of PCa. PCa is usually suspected when the plasma PSA concentration exceeds 4 ng/mL [4]. If an abnormality is found in the prostate by DRE, the next option is a biopsy and moleucular imaging *via* magnetic resonance imaging (MRI), computed tomography (CT), or ultrasound. However, these diagnostic methods have low selectivity and specificity for metastatic PCa. Additionally, increased PSA levels involving stimulation, such as ejaculation, have been reported [5]. Furthermore, PSA levels are elevated in benign diseases, such as benign prostatic hyperplasia and prostatitis [6]. The accuracy of the PSA test is not high with a sensitivity of 72.1%, a specificity of 93.2%, and positive predictive value of 25.1% [7]. Furthermore, PSA level does not provide information regarding the occurrence or site of metastasis.

1.2. Prostate-specific membrane antigen

Prostate-specific membrane antigen (PSMA) is a type II transmembrane protein that has physiological roles in the intestine, as folate hydrolase, and in the brain, as *N*-acetyl-L-aspartyl-L-glutamate peptidase (NAALADase) [8]. PSMA is distributed in the prostate, kidney, intestine, and brain. However, the level of PSMA expression in normal prostate cells is higher than that in the cells of other organs [9]. In addition, expression of PSMA gene in PCa cells is 8–12 times higher than in normal prostate cells [10].

PSMA acts as both a receptor and an enzyme, and internalizes and accumulates in the cytosol when bound to a

CONTACT Youngjoo Byun yjbyun1@korea.ac.kr Department of Pharmacy, College of Pharmacy, Korea University, 2511 Sejong-ro, Sejong 30019, South Korea; Song-Kyu Park spark123@korea.ac.kr College of Pharmacy, 2511 Sejong-ro, Sejong 30019, South Korea
[*] Equal contribution

Supplemental data for this article can be accessed here

Article Highlights

- PSMA is a type II transmembrane protein that is overexpressed in patients with metastatic prostate cancer.
- Hydrophilic PSMA-targeted inhibitors can easily access the PSMA active site in the extracellular region.
- Lys-urea-Glu is the most common motif for developing PSMA-targeted imaging or therapeutic probes.
- Bulky moieties including metal chelators, optical dyes, and cytotoxic agents have been successfully introduced by exploiting the tunnel region of the PSMA active site.
- This review covers 32 patents published from January 2017 to June 2020, describing small molecules based on the Lys-urea-Glu or Glu-urea-Glu structures.
- Most PSMA-targeted agents described in the patents demonstrated strong PSMA-inhibitory activities in the nanomolar IC50ranges and high tumor-to-background ratio (>5) in*ex vivo* and *in vivo experiments.*

ligand. For example, the PSMA-antibody complex is internalized through clathrin-coated pits and accumulates in the endosome [11]. PSMA possesses an active site in the extracellular region, which consists of three domains, and recognizes a substrate [12]. Therefore, the strategy for targeting PSMA as a diagnostic and therapeutic marker of metastatic PCa has some advantages, including facile access of hydrophilic PSMA-targeted probes to the extracellular PSMA active site, low membrane permeation, and low metabolic degradation in the cytosol [13].

For these reasons, PSMA-targeted inhibitors have been developed by mimicking the natural substrate of PSMA, *N*-acetyl-L-aspartyl-L-glutamate (NAAG). NAAG interacts with PSMA at the active site that consists of a glutamate-sensing pharmacophore S1′ pocket, non-pharmacophore S1 pocket, and two zinc (Zn) ions in the middle. A variety of amide bioisosteres, including urea [14–20], carbamate [21,22], phosphonate [23,24], and thiol groups [25,26] were introduced and interacted with two Zn ions in the PSMA active site. Among the bioisosteres, urea has been most commonly used. Particularly, lysine-urea-glutamate (Lys-urea-Glu) has been widely studied for the structural modification of PSMA-targeted inhibitors. The urea moiety of Lys-urea-Glu interacts with the Zn ions, forming stable hydrogen bonds with Tyr552 and Gly518. The Glu moiety of Lys-urea-Glu binds to the intolerant S1′ pocket consisting of Arg210, Asn257, and Lys699. The Lys moiety of Lys-urea-Glu mainly forms hydrogen bonds with Arg534, Arg536, and Asn519 in the S1 pocket. The S1 accessary pocket and the tunnel region close to the S1 pocket have been utilized to accommodate bulky prosthetic groups, optical dyes, cytotoxic agents, and linker moieties [15]. As shown in Figure 1(A), the potent PSMA inhibitor DCIBzL was found to form strong cation–π interactions in the S1 accessory pocket that consists of Arg463, Arg534, and Arg536 [16]. In the case of Lys-urea-Glu analogs conjugated with a linker or a bulky prosthetic group, the tunnel region and the remote arene-binding site on the surface area of PSMA have been utilized (Figure 1(B)). The remote arene-binding site is located at the entrance of the tunnel region that can be utilized to enhance binding affinity and modulate the hydrophilicity/hydrophobicity balance of the parent molecules [27,28]. Representative PSMA-targeted probes based on the Lys-urea-Glu motif include [^{18}F]DCFPyL [16], [^{18}F]PSMA-1007 [29], [^{68}Ga]Ga-PSMA-11 [30], and [^{177}Lu]Lu-PSMA-617 [31], which have successfully progressed into clinical phase trials (Figure 2). Recent clinical studies of [^{18}F]DCFPyL, [^{18}F]PSMA-1007, [^{68}Ga]Ga-PSMA-11, and [^{177}Lu]Lu-PSMA-617 have demonstrated that PSMA is a suitable target protein for metastatic PCa, demonstrating potential as a candidate compound for United States Food and Drug Administration (FDA) approval [30–34].

2. Patents on PSMA-targeted agents (2017–2020)

We attempted to classify the PSMA-targeted inhibitors disclosed in patents from January 2017 to June 2020. In particular, this review focuses on patents associated with PSMA inhibitors based on the Lys-urea-Glu or Glu-urea-Glu structures and describes the current state of discovery and development of PSMA-targeted agents.

2.1. Areas covered

This review describes progress in the field of PCa imaging and therapeutic probes targeting PSMA based on an analysis of PCT patent documents published from January 2017 to June 2020. Patents were searched in the European Patent Office (Espacenet) based on the inclusion of the keyword 'PSMA' in the title or abstract. In total, 83 patents were identified. However, only those patents that mentioned PCa diagnostic and treatment probes using Lys-urea-Glu or Glu-urea-Glu in their abstract or description were selected and summarized.

2.2. PSMA-targeted agents

The biological activities of the PSMA-targeted agents described in this review were determined under a variety of experimental conditions. Notably, *in vitro* assay systems and cell lines are needed to compare the activity among the reported compounds. For *in vitro* IC_{50} or K_i values, direct radioligand-based competitive assays and indirect fluorescence-based assays using Amplex red have been applied. In general, the K_i value of PSMA inhibitors is 4–8 times lower than the corresponding IC_{50} value. For cell lines, LNCaP, 22Rv1, and PC3 PIP cells expressing PSMA have been used. When assessing the tumor uptake of PSMA-targeted agents *in vitro* and *in vivo*, the level of PSMA expression in these cells should be considered before direct comparison of the %ID/g values. This is because, instead of the intrinsic properties of the imaging probes, the level of PSMA present in the cells can affect tumor uptake. PSMA expression in PC3 PIP cells was higher than that in LNCaP cells, while PSMA expression in 22Rv1 cells was lower than that in LNCaP cells [35,36]. Therefore, PSMA expression occurred in the following order: PC3 PIP, LNCaP, and 22Rv1 cells. C4-2 cells were reported to exhibit comparable mRNA PSMA expression to LNCaP cells

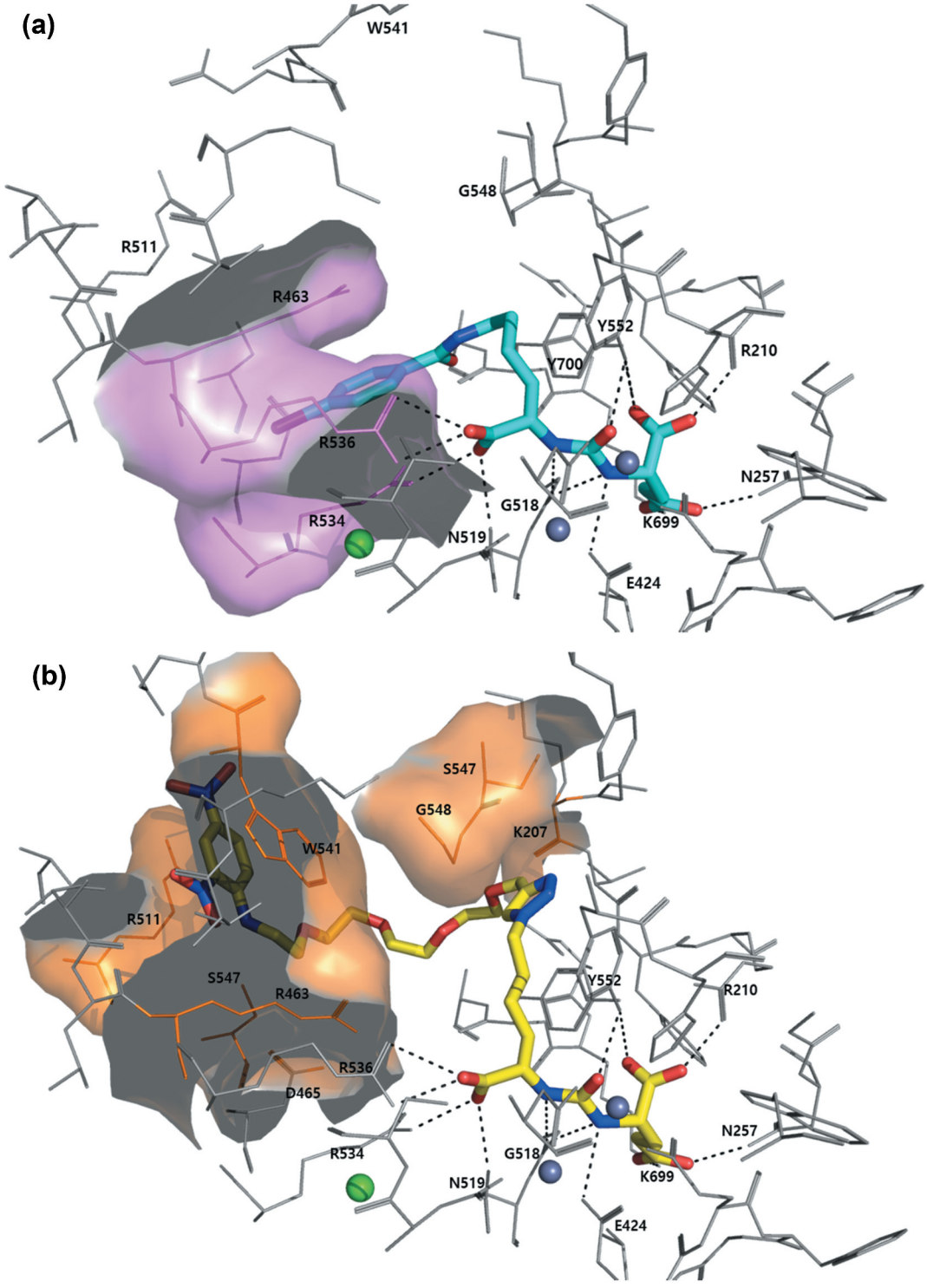

Figure 1. (A) PSMA S1 accessory pocket consisting of Arg 463, Arg 534 and Arg 536 (PDB ID: 3D7H), (B) Tunnel region and remote arene-binding site of PSMA (PDB ID: 2XEG).

[37]. *In vitro* assays and cell lines for each patent were added to Table 1.

2.2.1. PSMA-targeted imaging probes

Cellbion (KR) disclosed a PSMA inhibitor conjugated with NOTA or DOTA through a thiourea linker in WO2017082620 [38]. The PSMA inhibitor, [^{68}Ga]Ga-NOTA-SCN-GUL (**1**, Figure 3), was labeled with gallium-68 for PET imaging. The IC_{50} value of **1** was 18.3 nM. Biodistribution studies of **1** using BALB/c nude mice xenografted with 22Rv1 cells demonstrated moderate tumor uptake (5.40%ID/g) and a high tumor/blood ratio (31.76) at 1 h post-injection.

In patent WO2017027870, Johns Hopkins University (US) disclosed PSMA inhibitors that combined a triazole ring with a Lys-urea-Glu structure in the presence or absence of a PEG linker [39]. The representative compounds YC-71, YC-88 (**2**,

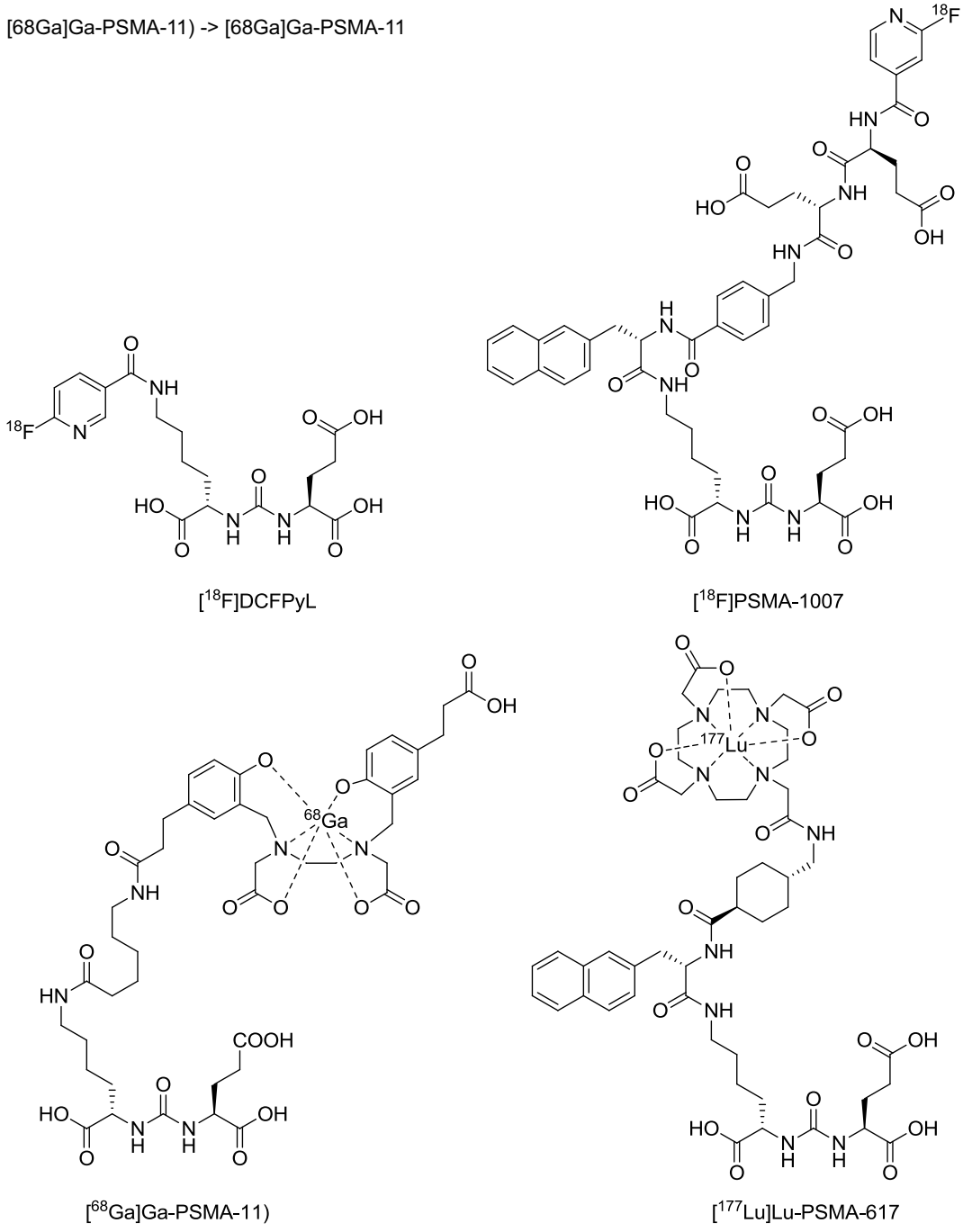

Figure 2. Representative PSMA-targeted agents in clinic trials.

Figure 3), and YC-XY-01 were labeled with fluorine-18. Their K_i values were 0.6, 12.9 and 473 nM, respectively. PET imaging and *ex vivo* biodistribution studies of **2** showed that the tumor uptake of PSMA+ PC3 PIP was 40.31, 47.58, 41.29, and 25.74% ID/g, at 0.5, 1, 2, and 4 h post-injection, respectively. The tumor/blood ratio was high, with values of 39.51, 164.1, 147.5, and 214.5, at 0.5, 1, 2, and 4 h, respectively.

The German Cancer Research Center and Heidelberg University (DE) disclosed 18 PSMA inhibitors labeled with fluorine-18 in patent WO2017054907 [40]. The IC_{50} values of the reported inhibitors were within the range of 4–14 nM. The representative compound PSMA-1007 (**3**, Figure 3) demonstrated strong PSMA-inhibitory activity with an IC_{50} value of 5 nM. The binding conformation of **3** in the PSMA active site was reported, presenting the interaction between the 2-fluoropyridine moiety of **3** and the remote arene-binding site [28]. With compound **3**, the LNCaP tumor uptake was 8%ID/g at 1 h post-injection in an *in vivo* and *ex vivo* biodistribution study. Compound **3** was also administered to healthy participants and patients with PCa who

underwent PET imaging studies. The maximum standardized uptake value (SUV_{max}) of **3** in patients was approximately 27 at 1 h post-administration.

Five Eleven Pharma (US) has released 16 PSMA inhibitors chelated with gallium-68 in patent WO2017116994 [41]. The IC_{50} values for these inhibitors were within the range of 5.0–132 nM, and compound 5b (**4**, Figure 3) presented an IC_{50} of 11.6 nM. Compound **4** labeled with gallium-68 was injected into control and LNCaP-xenografted mice. The tumor uptake of **4** was 11.26%ID/g and the tumor/blood ratio was 24.47 at 1 h post-injection.

In patent WO2017117687, The British Columbia Cancer Agency Branch and the University of British Columbia (CA) published seven PSMA inhibitors using the BF_3 moiety to introduce fluorine-18 [42]. PSMA inhibitors were administered to mice carrying LNCaP tumors, who were then used for PET/CT imaging and *ex vivo* biodistribution studies. *In vivo* tumor uptake of [^{18}F]HTK-01070 (**5**, Figure 3) was 8.28 and 7.56%ID/g at 1 and 2 h post-injection, respectively. The tumor/blood ratios were 16.0 and 38.9 at 1 and 2 h post-injection, respectively.

Dextech Medical AB (SE) disclosed a PSMA inhibitor conjugating a guanidine-dextran with the Lys-urea-Glu structure in patent WO2017220488 [43]. Imaging studies were performed after administration of a FITC-labeled inhibitor to 22Rv1 tumor cells. The gadolinium-labeled DOTA-substituted inhibitor (**6**, Figure 3) was also disclosed in the patent. However, detailed results from *in vivo* studies were not included.

Cornell University (US) disclosed six PSMA inhibitors in patent WO2018005625 containing a triazole moiety that were prepared using click chemistry and were labeled with fluorine-18 [44]. PET/CT imaging of mice carrying LNCaP tumors was performed to evaluate biodistribution. Compounds RPS-040 (**7**, Figure 3) and RPS-041 presented IC_{50} values of 7.0 and 3.2 nM, respectively; however, the tumor uptake of **7** and RPS-041 was 14.30 and 10.86%ID/g at 2 h post-administration, respectively. These results imply that *in vitro* IC_{50} and *in vivo* tumor uptake are not exactly proportional to each other [20]. Notably, there was a strong correlation between *in vitro* internalization and *in vivo* tumor uptake [45,46].

The Memorial Sloan Kettering Cancer Center (US) disclosed PSMA inhibitors that conjugate C Dot (macromolecule) with a Lys-urea-Glu structure in WO2018102372 [47]. Heterodimeric constructs of NOTA-PSMAi-C Dot (**8**, Figure 3) and GRP-DOTA peptides were designed to enhance binding affinity to cell lines to express both PSMA and gastrin-releasing peptide receptor (GRPr). Compound **8** labeled with copper-64 was stable in water, saline, and serum. [^{64}Cu]**8** was internalized in LNCaP cells bound to PSMA but blocked by treatment with the potent PSMA inhibitor, 2-(phosphonomethyl)pentanedioic acid (PMPA). Using compound **8** labeled with gallium-67, tumor and kidney uptake was approximately 3.5 and 2.5%ID/g, respectively, at 24 h post-injection.

In patent WO2018215627, Isotope Technologies Munich AG (DE) disclosed a PSMA inhibitor that consists of the Lys-urea-Glu structure, an albumin-binding entity, a linker, and a chelator. This inhibitor PSMA-ALB-89 (**9**, Figure 3) was labeled with copper-64 [48]. Although lipophilic 2-naphtyl-L-alanine and 4-iodobenzyl moieties were introduced, compound **9** remained hydrophilic and had a low logD value of −2.3 and plasma albumin binding of >92%. The uptake of **9** into PMSA+ PC-3 PIP cells was ~46% following 2 h incubation at 37°C, whereas the uptake of **9** into PSMA-PC3 flu cells was <0.5%. Accumulation of **9** in PSMA+ PC3 PIP tumors was high at 1 h. The tumor/blood ratio was 31.3 at 24 h post-injection.

Futurechem (KR) disclosed nine PSMA inhibitors in patent WO2018236115 [49]. PSMA inhibitors labeled with fluorine-18 were administered to 22Rv1 cells. The IC_{50} value of the inhibitor, designated [^{18}F]I-6 (**10**, Figure 3), was 5.08 nM. The triazole and pyridine moieties of the **10** analogs increased the hydrophilicity of the parent molecule, resulting in a decrease in nonspecific binding in off-target organs, such as the liver and spleen. Biodistribution was measured following injection of **10** to mice with PSMA+ PC3 PIP tumors, and to mice with PSMA- PC3 flu tumors. The PIP tumor/blood ratio of **10** was 30.3 at 1 h post-injection.

University of Cologne (DE) disclosed five PSMA inhibitors in patent WO2019175405 [50]. Data on the uptake of representative compounds 2-MeO-[^{18}F]PSMA (**11**, Figure 3) and 4-MeO-[^{18}F]PSMA from PSMA+ LNCaP C4-2 cells were obtained. The cellular uptake of **11** and [^{18}F]DCFPyL was 2.03 and 1.55%ID/10^5 cells at 2 h, and 3.31 and 3.1%ID/10^5 cells at 4 h, respectively. Accumulation of **11** in organs, including the superior cervical ganglion, was confirmed in PET imaging study. In a clinical study of 124 patients with biochemical recurrence of PCa, **11** demonstrated 83.0% sensitivity compared to 79.1 and 74.2% for [^{18}F]DCFPyL and [^{68}Ga]Ga-PSMA-HBED-CC (see supplementary material), respectively [51].

Futurechem (KR) reported 16 PSMA inhibitors in patent WO2019190266 [52]. The IC_{50} and K_i values of the ^{68}Ga-labeled inhibitors were assessed using 22Rv1 cell lines. The IC_{50} values of the inhibitors [^{68}Ga]Ga-1e, [^{68}Ga]Ga-1g, [^{68}Ga]Ga-1h (**12**, Figure 3), and [^{68}Ga]Ga-1k were 47.41, 18.40, 11.00, and 63.85 nM, respectively (see supplementary material). The tumor uptake of [^{68}Ga]Ga-1e, [^{68}Ga]Ga-1g, **12**, and [^{68}Ga]Ga-1k was 4.73, 8.29, 7.90, and 5.45%ID/g at 1 h post-injection, respectively. The logP values for these inhibitors determined by counting the radiation dose in *n*-octanol and PBS buffer solution were within the range of −1.89 to −3.06, indicating that the compounds are highly hydrophilic.

Heidelberg University and German Cancer Research Center (DE) disclosed 18 PSMA inhibitors in patent WO2020065045 [53]. The K_i values of these inhibitors were in the range of 1.60 nM to 33.82 nM, The K_i value of the representative compound [^{64}Cu]Cu-CA003 (**13**, Figure 3) was 1.60 nM. When **13** was administered to mice bearing C4-2 tumors, high tumor uptake was observed, with 11, 31, 32, 20, and 4%ID/g at

10 min, 1, 4, 24, and 72 h post-injection, respectively. Following the administration of 200 MBq **13** to a patient, PET images were able clearly to detect the site of metastasis.

National Institute for Nuclear Research (MX) disclosed one PSMA inhibitor, named [^{99m}Tc]Tc-EDDA/HYNIC-iPSMA (**14**, Figure 3), in patent WO2017222362 [54]. This inhibitor consists of a Lys-urea-Glu structure, hydrazononicotinamide (HYNIC), and [^{99m}Tc]Tc-EDDA as a moiety for single-photon emission computed tomography (SPECT). The HYNIC moiety increased the lipophilicity and binding affinity of the parent molecule to PSMA. The IC_{50} value of compound **14** was 2.9 nM. Biodistribution was measured by administering **14** to mice carrying LNCaP tumors, and the tumor uptake was 8.7%ID/g. [^{68}Ga]Ga-PSMA-617 and **14** were administered to healthy participants and patients. The sensitivity of [^{99m}Tc]Tc-**14** SPECT images was as high as that of PET images using [^{68}Ga]Ga-PSMA-617.

2.2.2. PSMA-targeted therapeutic agents

In patent WO2017070482, Johns Hopkins University and Duke University (US) disclosed 16 PSMA inhibitors [55]. The K_i values of YC-I-27 and HS-549 were 0.01 and 0.01 nM, respectively. [^{211}At]YC-I-27 (**15**, Figure 4) was presumed to interact with the S1 accessory pocket of the PSMA active site. Tumor uptake was determined following the administration of **15** to mice bearing PSMA+ PC3 PIP and PSMA- PC3 flu tumors. Compound **15** demonstrated higher uptake into PSMA+ PC3 PIP tumors (17.9, 20.7, 18.3, and 31.1%ID/g at 1, 2, 4, and 18 h, respectively) compared to PSMA- PC3 flu tumors (2.18, 1.81, 1.53, and 1.17%ID/g at 1, 2, 4, and 18 h). The PSMA+ PC3 PIP tumor/blood ratio was 10.7, 16.4, 18.5, and 58.7 at 1, 2, 4, and 18 h post-injection, respectively. The PIP tumor/kidney ratios were 0.25, 0.34, 0.30, and 0.52 at 1, 2, 4, and 18 h, respectively. When **15** was administered to mice bearing PSMA+ PC3 PIP tumors, tumor growth was inhibited. Mice treated with **15** presented a slight increase in tumor size from about 2 to 4 mm^3. However, the tumor size in the control group greatly increased from about 2 to 16 mm^3 under the same experimental conditions.

In patent WO2019157037, Johns Hopkins University (US) reported a variety of theranostic PSMA inhibitors in collaboration with Duke University. They focused on evaluating an inhibitor, termed [^{211}At]VK-02-90-Lu (**16**, Figure 4) [56]. Biodistribution studies using athymic mice with PSMA+ PC3 PIP and PSMA- PC3 flu tumors demonstrated high tumor uptake of 30.6, 17.1, and 9.5%ID/g at 1, 4, and 24 h post-injection, respectively. Kidney uptake was 90, 2.1, and 0.02% ID/g at 1 h, 4 h, and 24 h, respectively. The tumor size and median survival time were also determined following the administration of **16** to athymic mice. Compound **16** did not have a significant effect on tumor growth inhibition in PSMA-PC3 flu-xenografted mice. However, tumor growth was suppressed in PSMA+ PC3 PIP-xenografted mice. Furthermore, as the dose of **16** increased, the median survival time of mice increased. The median survival time after treatment with **16** (1.48 MBq) was approximately 39 days, whereas that of **16** (3.7 MBq) was more than 50 days.

Cornell University (US) reported eight PSMA inhibitors in WO2017223357 [57]. The IC_{50} value of the representative compound RPS-005 (**17**, Figure 4) was 4 nM. It is expected that the 3-(4-iodophenyl)propyl moiety of **17** interacts with the tunnel region rather than the S1 accessary pocket. Compound **17** and its analogs (see supplementary material) were labeled with iodine-131 and administered to mice xenografted with PSMA+ LNCaP tumors. Compound [^{131}I]**17** showed high uptake in LNCaP tumors, with 9.37 and 10.82% ID/g at 24 and 96 h post-injection, respectively. The tumor/kidney uptake ratio at 24 h was 0.24.

ITM Isotope Technologies Munich AG (DE) reported seven PSMA inhibitors in patent WO2018233798 [58] that consisted of a Lys-urea-Glu structure, an albumin-binding entity, a linker, and a chelator group. Biodistribution was assessed by administering a ^{177}Lu-labeled inhibitor to mice bearing PSMA+ PC3 PIP and PSMA-PC3 flu tumors. The tumor/blood ratios of [-^{177}Lu]Lu-PSMA-ALB-06 (**18**, Figure 4) and [^{177}Lu]Lu-PSMA-ALB-08 were high with values of 77.6 and 421%ID/g at 24 h post-injection, respectively. The tumor/kidney ratio was 10.4 and 2.39 at 24 h post-injection, respectively.

The British Columbia Cancer Agency Branch and University of British Columbia (CA) collaborated to report 15 PSMA inhibitors in patent WO2019075583 [59]. The K_i value of [^{177}Lu]Lu-HTK01169 (**19**, Figure 4) was 0.04 nM. The tumor uptake of **19** was 55.9%ID/g and the tumor/blood ratio was 26.7 at 24 h post-injection. The tumor/kidney ratio of **19** was 0.45 at 24 h. Furthermore, in mice bearing LNCaP tumors, the median survival time and tumor volume were measured according to the radiation dose of **19**. The median survival time increased as the dose of **19** increased. The median survival time of mice treated with 18.5 MBq **19** was >120 days, whereas that of mice treated with 2.3 MBq **19** was 28 days.

Sciencons AS (NO) disclosed two PSMA inhibitors in patent WO2019115684 [60]. Biodistribution was measured by administering ^{212}Pb-labeled PSMA inhibitors to mice with PSMA+ PC3 PIP tumors. Among the inhibitors, [^{212}Pb]Pb-p-SCN-Bn-TCMC-PSMA-1(**20**, Figure 4) exhibited high tumor uptake of 15.87%ID/g and a tumor/blood ratio of 29.4 at 2 h post-injection. The tumor/kidney ratio of **20** was 0.62 at 2 h. The median survival time was determined by administering **20** to mice xenografted with PSMA-positive C4-2 tumors. Each group of eight mice was treated with saline, [^{177}Lu]Lu-PSMA-617, or **20** for 30 days. The median survival time of mice treated with saline was only 15 days, while that of mice treated with [^{177}Lu]Lu-PSMA-617 was 20 days. However, the median survival time of mice treated with **20** was considerably high, at more than 30 days. In terms of radiation dose, [^{177}Lu]Lu-PSMA-617 was higher than **20** (35.9 Gy for [^{177}Lu]Lu-PSMA-617 and 2.06 Gy for **20**). Beta particle lead-212 (physical half-life: 10.64 h) decays to produce ^{212}Bi and ^{212}Po, generating alpha particle radiation. Alpha-emitting particles have high linear energy transfer (>100 keV/μm) and a short radiation range in tissue (<0.1 mm) that can effectively kill cancer cells and reduce the side effects in surrounding normal cells.

Technical University of Munich (DE) released 11 PSMA inhibitors in patent WO2019115547 [61]. The IC_{50} values of [^{177}Lu]Lu-PSMA-62 (**21**, Figure 4) and [^{177}Lu]Lu-PSMA-66 were 4.0 and 3.8 nM, respectively. The LNCaP tumor uptake of **21** and [^{177}Lu]Lu-PSMA-66 was 7.70 and 5.73%ID/g at 24 h post-injection, and the tumor/blood ratios were 1925 and 1910,

respectively. The tumor/kidney uptake ratio was 1.5 and 0.3 at 24 h, respectively. Detailed *in vivo* data, including the median survival time and tumor growth inhibition, were not reported in the patent.

US Health (US) reported PSMA inhibitors conjugated with Evans Blue (EB) dye in patent WO2019165200 [62]. The IC_{50} values of EB-PSMA-617 (**22**, Figure 4), EB-MCG, and DOTA-MCG were 7.2, 18.5, and 104.7 nM, respectively. The inhibitors were radiolabeled with yttrium-86, yttrium-90, or lutetium-177 and administered to mice carrying PSMA+ PC3 PIP tumors. The tumor and kidney uptake AUC of [^{86}Y]**22** was 1268 and 493 μg·h/mL, respectively. Then, compound **22** labeled with yttrium-90 or lutetium-177 was administered to determine the median survival time and change in tumor volume. The tumor volume increased following the administration of saline, [^{177}Lu]Lu-PSMA-617, or [^{90}Y]Y-PSMA-617, respectively. All saline-treated mice died before day 20. In the case of [^{177}Lu]Lu-PSMA-617, all mice died before day 50. Following administration of the positive control compounds, including [^{90}Y]Y-DOTA-MCG and [^{177}Lu]Lu-DOTA-MCG, the tumors were not resolved, and all mice died within 20–30 days. However, the tumor decreased substantially in size, and all mice survived for more than 120 days when [^{90}Y]**22** or [^{177}Lu]**22** was administered.

National Institute for Nuclear Research (MX) disclosed one PSMA inhibitor, named [^{177}Lu]Lu-DOTA-HYNIC-iPSMA (**23**, Figure 4), in patent WO2019177499 [63], consisting of a Lys-urea-Glu structure, HYNIC and ^{177}Lu-DOTA. The K_d value of the inhibitor was 6.33 nM. Biodistribution was measured by administering **23** to mice bearing LNCaP tumors. The tumor uptake was 9.74%ID/g. Eleven patients were treated with **23** (3.7 or 7.4 GBq), and the response was confirmed by PET imaging with [^{68}Ga]Ga-PSMA-11. PSA levels were decreased and the number and size of metastatic lesions were reduced in 60% of the patients.

2.3. PSMA-targeted agents conjugated with an optical dye or a cytotoxic molecule

In patent WO2018232280, Johns Hopkins University (US) disclosed 10 PSMA optical imaging probes, obtained by conjugating the Lys-urea-Glu structure with an NIR dye (800 nm wavelength) [64]. Although the exact IC_{50} or K_i values were not provided, *in vivo* and *ex vivo* imaging studies were performed. The tumor uptake of two compounds (Dylight800-1 and Dylight800-2) without a linker was lower than the other compounds containing a linker. Dylight800-3 ~ Dylight800-10 with a linker exhibited high tumor uptake. However, Dylight800-7 ~ Dylight800-10 (**24**, Figure 5) with a PEG linker had lower renal uptake than Dylight800-3 ~ Dylight800-6 with a suberic acid linker, demonstrating a significant effect of the linker property on the *in vivo* distribution profile. Among them, compound **24** with a PEG linker and 4-bromobenzyl moiety demonstrated the most favorable *in vivo* profiles including the highest tumor uptake and low renal uptake.

On Target Laboratories LCC (US) disclosed 147 PSMA inhibitors in patent WO2017044584 [65], comprising a B-X-Y-Z general structure. B is a Glu-urea-Glu structure that anchors PSMA; X is a hydrophobic spacer; Y is an amino acid spacer; and Z is an NIR dye. These new inhibitors utilized fluorescent NIR dyes for imaging, but not radioactive isotopes. The K_d values and fluorescent imaging of the inhibitors were determined using 22Rv1 tumor cells. The K_d values of the inhibitors ranged from 2.6 to 983 nM. The K_d value of compound 1 (**25**, Figure 5) was 141.9 nM. The tumor/kidney uptake ratio of **25** was approximately 1.0 at 2 h post-injection.

In patent WO2018049132, On Target Laboratories LCC (US) disclosed a PSMA inhibitor, named OTL78 (**26**, Figure 5), synthesized by combining an NIR dye with the Lys-urea-Glu structure [66]. Following administration of **26** to mice with 22Rv1 cells, biodistribution patterns were confirmed by optical imaging; however, the exact values were not reported.

Case Western Reserve University (US) disclosed four PSMA inhibitors conjugated with a cytotoxic molecule in patent WO2019183633 [67]. The cell viability IC_{50} values of PSMA-Cy5.5-MMAE (**27**, Figure 5) were 3.56 and 16.4 nM in PSMA+ PC3 PIP and PSMA- PC3 flu cells, respectively. In the patent, monomethyl auristatin E (MMAE) and doxorubicin (Dox) were used as cytotoxic substances. MMAE inhibits the division of tumor cells by blocking the polymerization of tubulin, while Dox blocks DNA transcription by inhibiting topoisomerase II. PSMA-1-MMCCH-Dox (see supplementary material) presented higher cytotoxicity to PSMA+ PC3 PIP tumors than PSMA- PC3 flu tumors. Mice implanted with PSMA+ PC3 PIP tumors were treated with free Dox or PSMA-1-MMCC-Dox in PBS solution. Tumors in mice treated with free Dox grew faster than those treated with PSMA-1-MMCC-Dox. In addition, mice treated with PSMA-1-MMCC-Dox showed less weight loss than control.

Endocyte (US) disclosed three PSMA inhibitors in patent WO2017205447 [68], including EC0652, which was labeled with technetium-99m and administered to patients for diagnosis. Patients were then treated with a PSMA ligand-tubulysin conjugate (**28**, Figure 5). Tubulysin is a highly cytotoxic peptide with antimitotic activity. Sixteen of the 72 patients treated with **28** were stable for at least three months. Several dose-limiting toxicities, including hematological toxicity, neutropenia, thrombocytopenia, nausea, and vomiting, have been reported.

Heidelberg Pharma Research GmbH (DE) reported 22 PSMA inhibitors that connect the Lys-urea-Glu with a cytotoxic molecule (amatoxin) in patent WO2019057964 [69]. Amatoxin, a poison found in some mushrooms, selectively inhibits RNA polymerase II. Cytotoxicity of the representative inhibitors, HDP30.2284 and HDP30.2301 (**29**, Figure 5), were determined using PSMA+ LNCaP and PSMA- PC3 cells. The cell viability IC_{50} values of HDP 30.2284 and **29** were 0.86 and 6.11 nM in LNCaP cells, whereas those in PC3 cells were 1570 and 1520 nM, respectively. LNCaP, 22Rv1, and PC3 tumor cells were treated with these PSMA inhibitors to confirm the cytotoxicity of **29**. The EC_{50} of **29** in LNCaP, 22Rv1, and PC3 tumor cells was approximately 8.4 nM, 301 nM, and 3 μM, respectively. In addition, an antibody fragment, Fc-LPETG, was linked to a PSMA inhibitor and then administered to mice xenografted with LNCaP tumors to confirm its therapeutic effect. The tumor was resolved on day 25 following administration of the inhibitor once a week at 1 mg/kg or twice a week at 0.5 mg/kg. Tumor growth was also suppressed when the inhibitor was administered twice a week at 0.25 mg/kg.

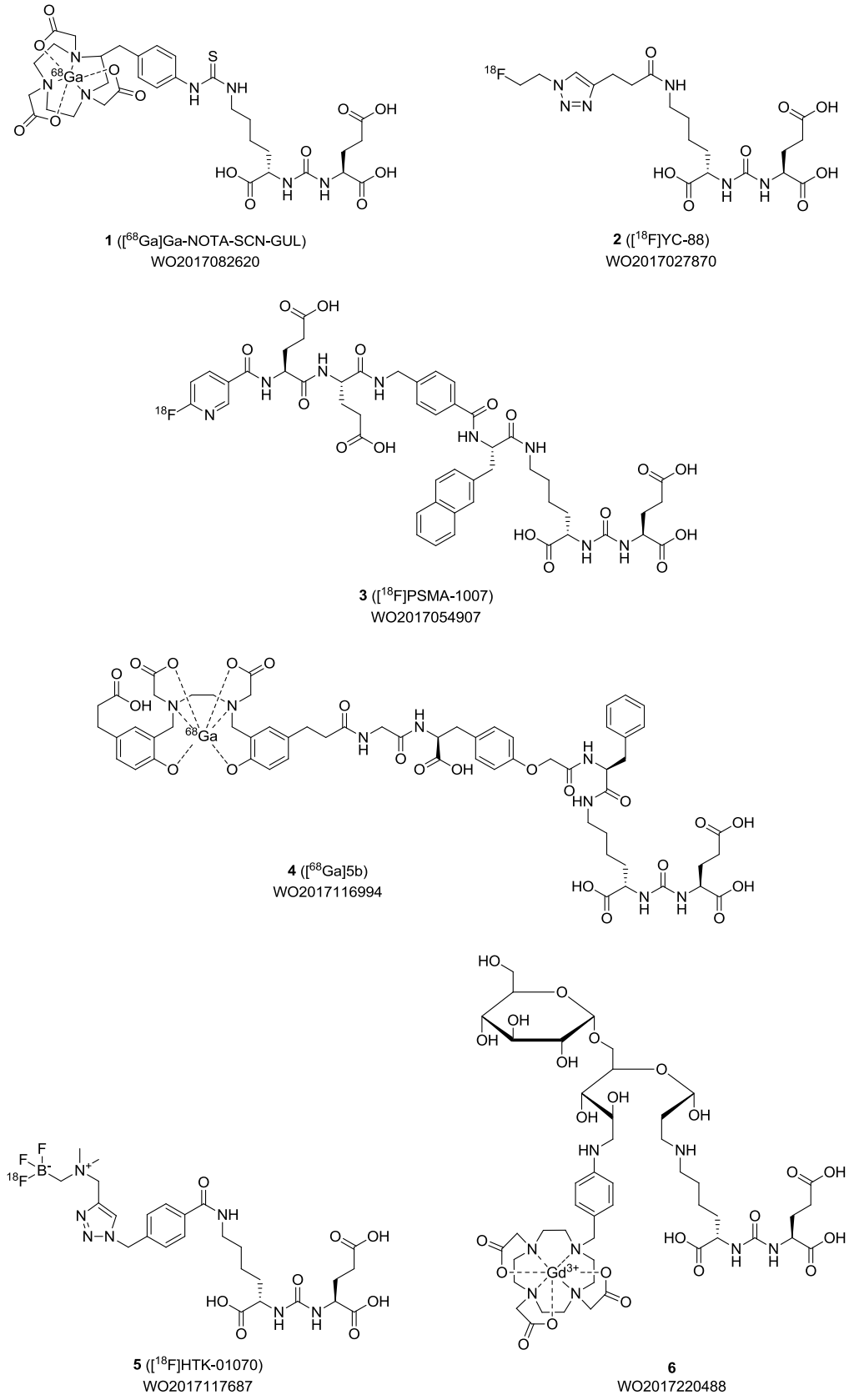

Figure 3. PSMA-targeted imaging probes.

In patent WO2018098390, Cancer Targeted Technology LLC (US) disclosed PSMA inhibitors conjugated to an albumin-binding moiety based on the structures of DOTA and Lys-urea-Glu, without the inclusion of any *in vitro* or *in vivo* data

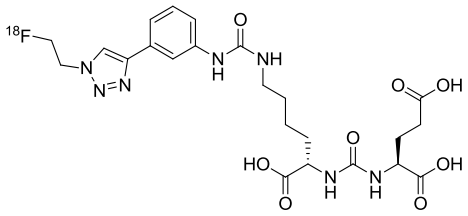

7 ([^{18}F]RPS-040)
WO2018005625

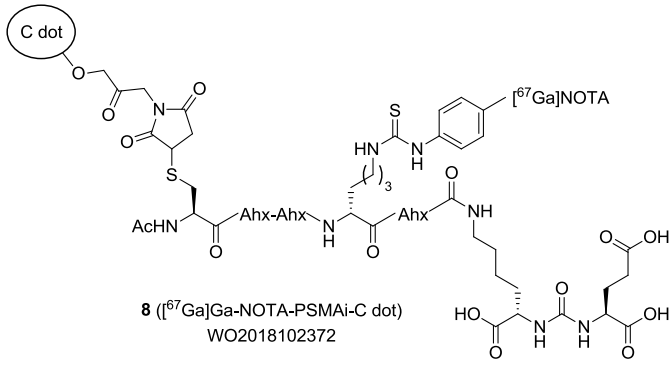

8 ([^{67}Ga]Ga-NOTA-PSMAi-C dot)
WO2018102372

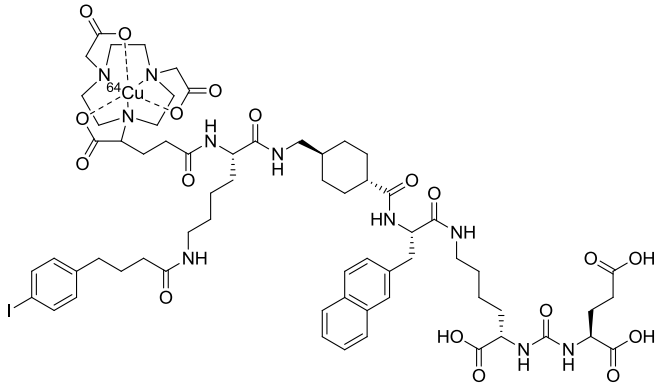

9 ([^{64}Cu]Cu-PSMA-ALB-89)
WO2018215627

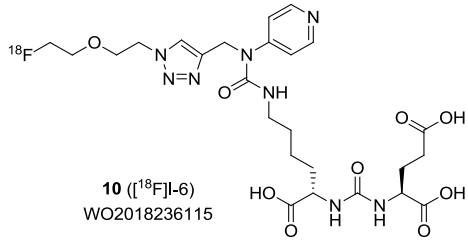

10 ([^{18}F]I-6)
WO2018236115

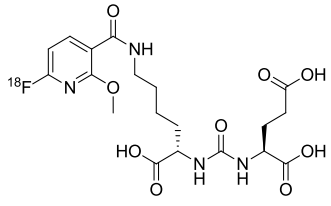

11 (2-MeO-[^{18}F]PSMA)
WO2019175405

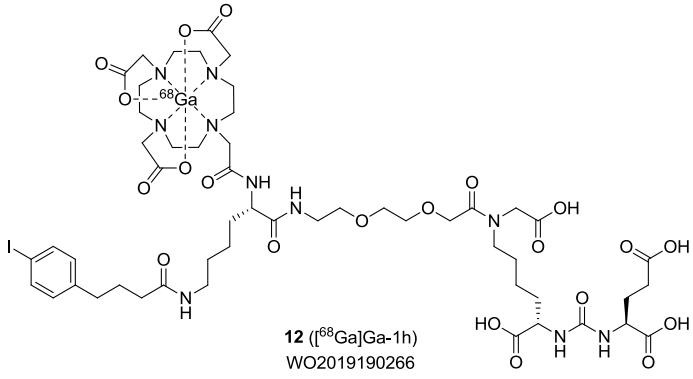

12 ([^{68}Ga]Ga-1h)
WO2019190266

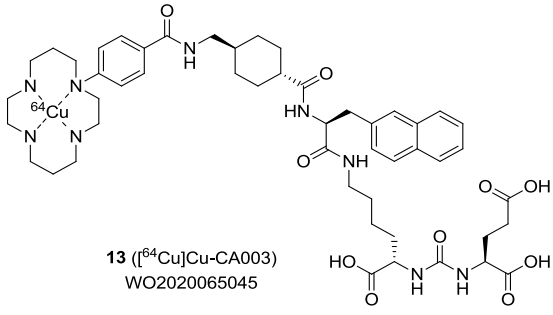

13 ([^{64}Cu]Cu-CA003)
WO2020065045

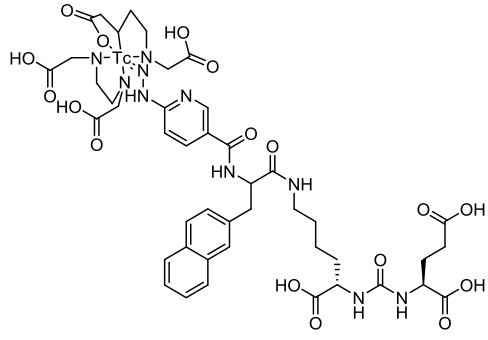

14 ([^{99m}Tc]Tc-EDDA/HYNIC-iPSMA)
WO2017222362

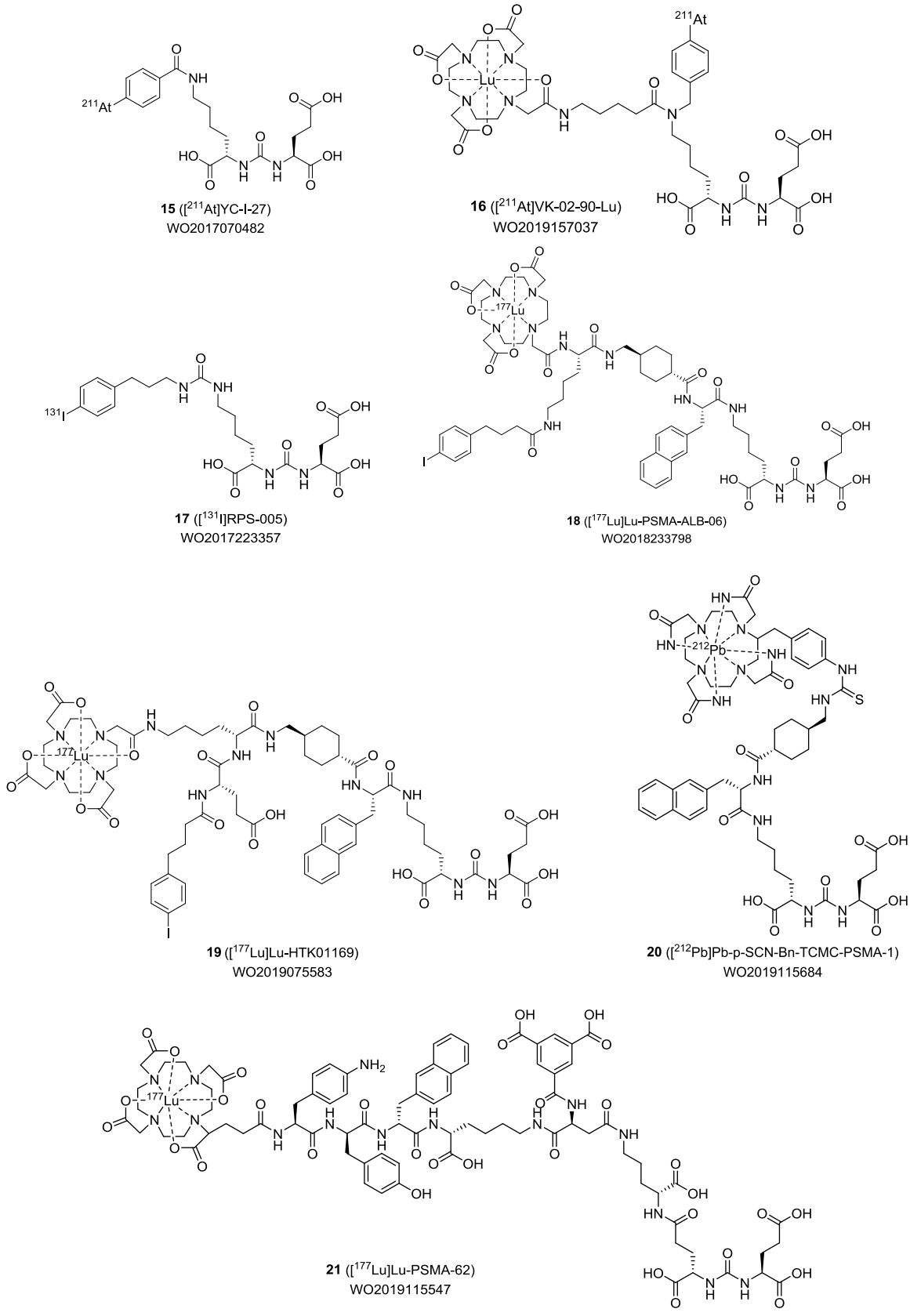

Figure 4. PSMA-targeted therapeutic agents.

[70]. The 4-iodophenylalkyl group was reported as an albumin-binding moiety to develop long-acting therapeutic agents [71].

In patent WO2020028324, Johns Hopkins University (US) disclosed PSMA-targeted phototheranostic agents termed LC-pyro (**30**, Figure 5) and SC-Pyro that comprised a porphyrin-

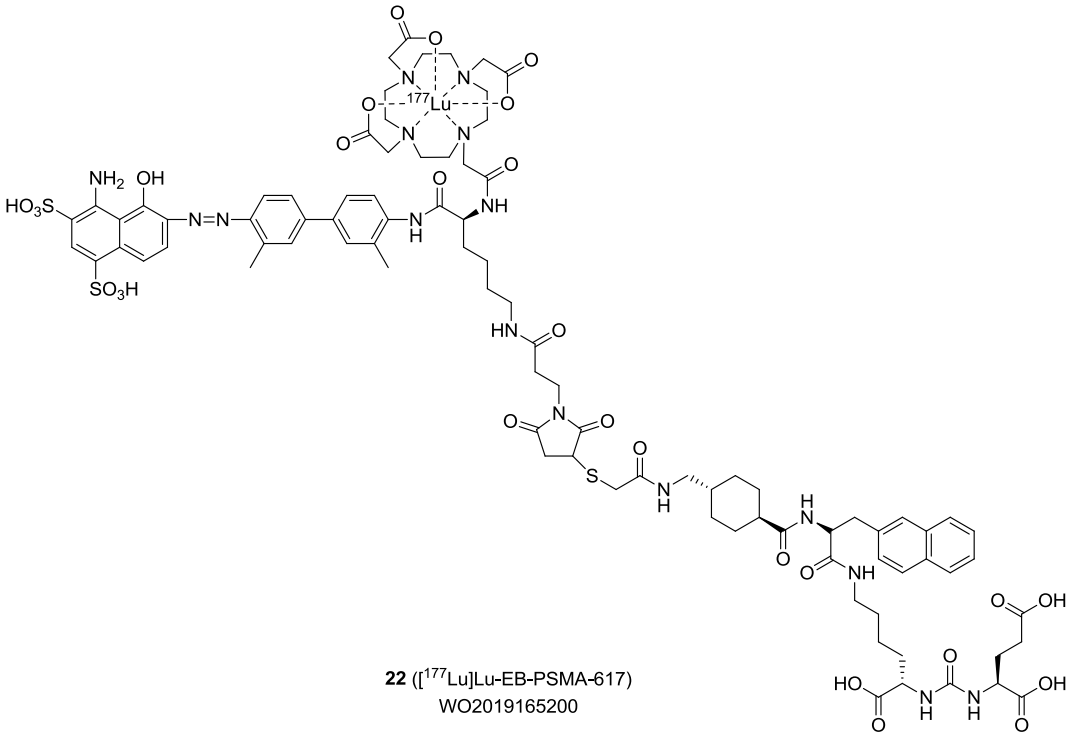

22 ([^{177}Lu]Lu-EB-PSMA-617)
WO2019165200

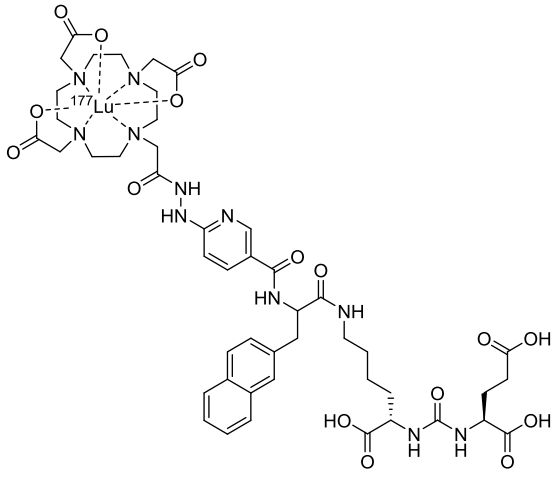

23 ([^{177}Lu]Lu-DOTA-HYNIC-iPSMA)
WO2019117499

based photosensitizer and a Lys-urea-Glu structure [72]. Based on the results of an *in vitro* fluorescence-based assay, these compounds were found to be potent PSMA inhibitors with K_i values of 0.088 and 0.2 nM, respectively. In particular, compound **30** labeled with copper-64 presented four-fold higher uptake in PSMA+ PC3 PIP tumors, with 9.74%ID/g at 17 h post-injection, than that of the PSMA- PC3 flu tumor (2.30%ID/g). The tumor/blood ratio was 4.14 at 17 h post-injection. Following the administration of **30** to PSMA+ PC3 PIP-bearing mice in combination with laser for photodynamic therapy, the mice were cured after 22 days. However, no therapeutic effect was observed in the case of compound **30** only in the absence of laser or laser alone.

Korea University (KR) disclosed 16 PSMA inhibitors based on β- or γ-amino acids in patent WO2020080842 [73]. The IC_{50} value of the most potent compound 16c (**31**, Figure 5) was 3.97 nM. The PSMA X-ray crystal structure in complex with **31** (PDB ID: 6RBC) explained the binding mode of the β-amino acid analog, demonstrating the flexibility of the S1 pocket and tunnel region [18]. However, detailed information on **31**, such as radiolabeling and *in vivo* data, was not included in the patent.

3. Conclusions

This review discusses 32 patents for PSMA-targeted imaging and therapeutic agents based on the Lys-urea-Glu or Glu-urea-Glu structure, published from January 2017 to June 2020 (Table 1). Most of the patented PSMA-targeted agents presented strong PSMA-inhibitory activity with IC_{50} or K_i values in the nanomolar range and high tumor/blood ratio (>5) in *in vivo* and *ex vivo* experiments. Structural changes in the

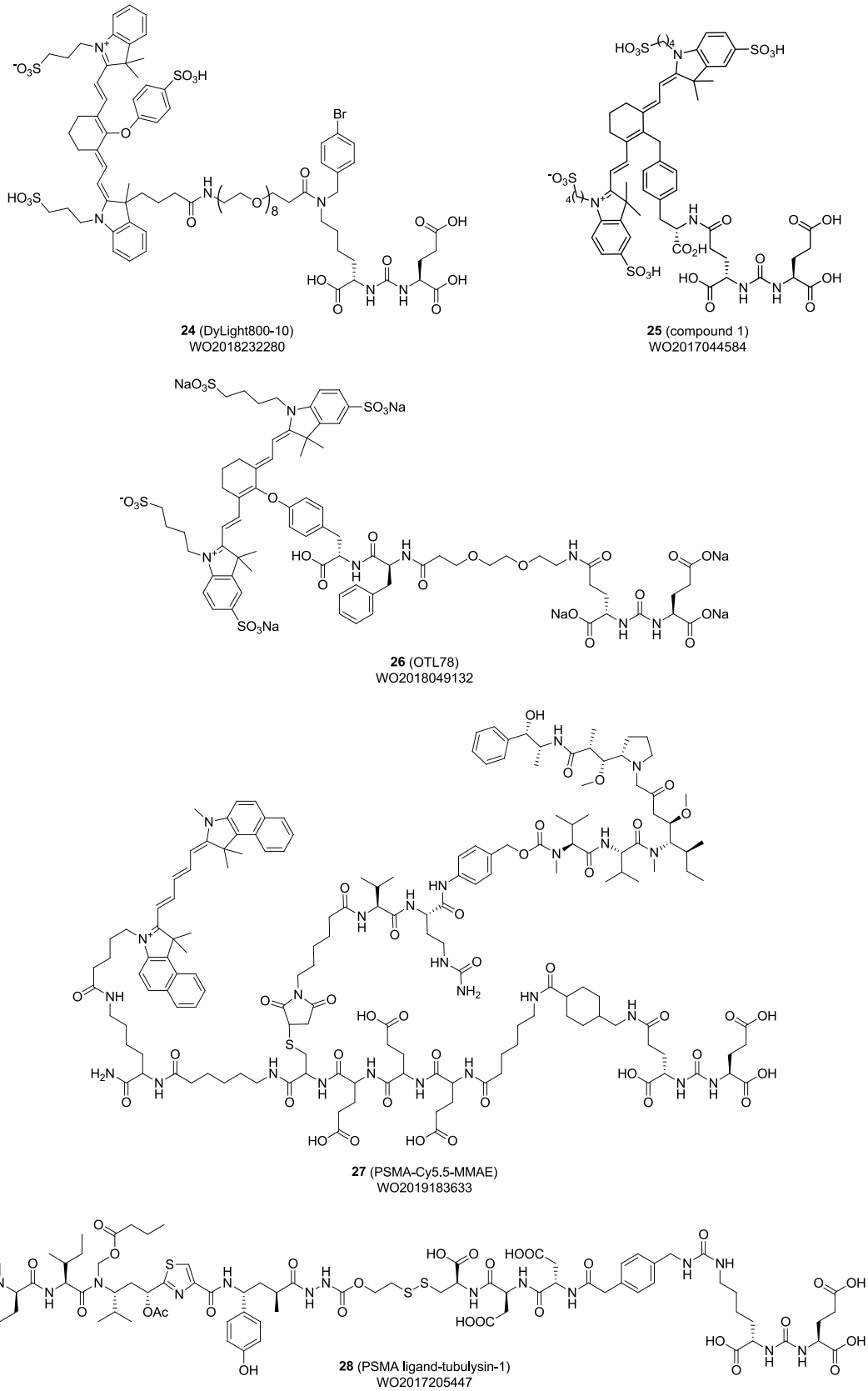

Figure 5. Miscellaneous PSMA-targeted agents.

patented compounds were found on the S1 accessory pocket and tunnel region, keeping the glutamate-binding S1′ site unchanged. Notably, the optimization of the linker and introduction of radiometal-chelating moieties was achieved by utilizing the flexibility of the tunnel region. For the diagnosis of metastatic PCa, PET imaging probes radiolabeled with

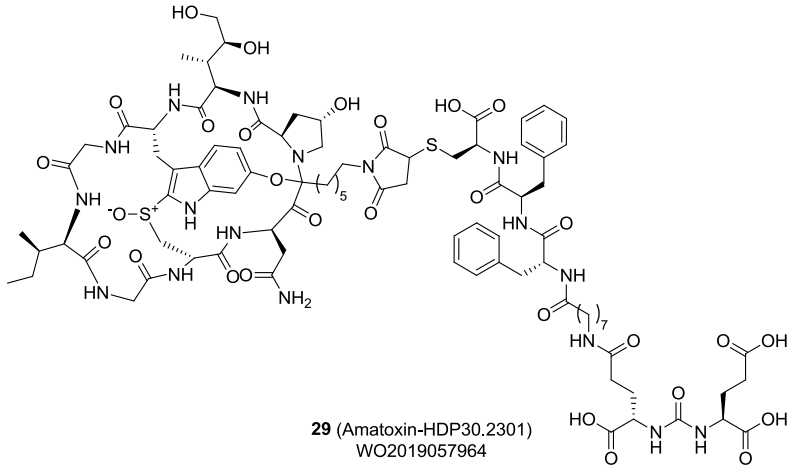

29 (Amatoxin-HDP30.2301)
WO2019057964

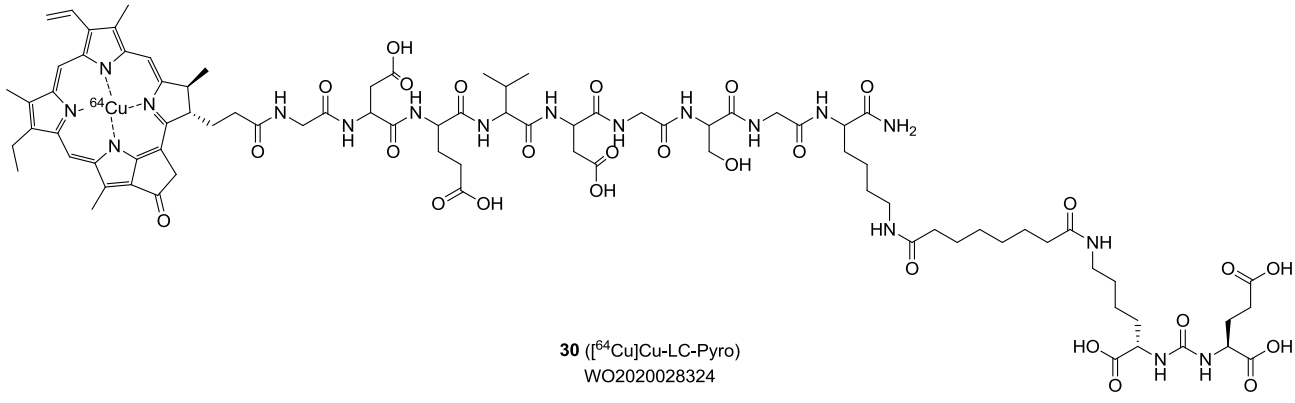

30 ([^{64}Cu]Cu-LC-Pyro)
WO2020028324

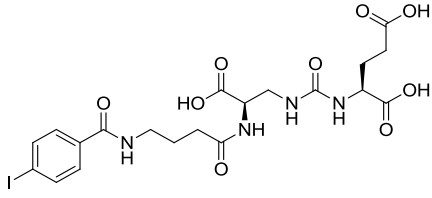

31 (16c)
WO2020080842

fluorine-18, copper-64, and gallium-68, as well as SPECT probes labeled with technetium-99m, have demonstrated promising results in animal and human studies. Therapeutic agents labeled with α- or β-emitting radionuclides have increased the median survival time and decreased tumor size in *in vivo* experiments. In addition, conjugate compounds that link Lys-urea-Glu with cytotoxic agents have been synthesized and evaluated for their anti-tumor activities.

4. Expert opinion

PSMA is a type II transmembrane protein that is an attractive target for the diagnosis and therapy of patients with metastatic PCa [74–76]. Since PSMA functions as both an enzyme and a receptor, these two roles must be considered when discovering and developing drugs that target PSMA. Particularly, the location of the active site in the extracellular region provides several advantages for the structural modification of PSMA inhibitors derived from Lys-urea-Glu or Glu-urea-Glu motifs. As Lys-urea-Glu and Glu-urea-Glu contain three carboxylic acids in their structure, the parent molecule is highly hydrophilic and cannot easily cross lipophilic cell membranes. Therefore, hydrophilic PSMA inhibitors targeting the extracellular active site do not have problems such as cell membrane permeation and metabolic degradation in the cytosol.

The tumor-to-background ratio is a key factor in determining the success of imaging probes targeting PSMA. As PSMA is expressed in the intestine, brain, and the kidney, the uptake of PSMA-targeted probes into PSMA-expressing tumors should be higher than that into background regions (blood, muscle, and kidney) for successful imaging and treatment [77,78]. Since the kidney is a major off-target organ, some efforts have been made to minimize renal uptake without limiting the tumor dose. Co-administration of 2-PMPA (0.2–1.0 mg/kg) with a radiolabeled PSMA inhibitor has demonstrated promising results in limiting renal uptake while maintaining tumor

Table 1. Summary of representative compounds in the patents (Jan 2017 – Jun 2020)

PCT Number	Applicant	Representative compound	assay	IC_{50}(nM)[a] K_i(nM)[b]	Tumor uptake (%ID/g)	Tumor/Blood ratio[c] Tumor/Muscle ratio[d] Tumor/Kidney ratio[e]	Reference
WO2017/082620	Cellbion	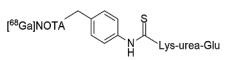	[^{125}I]MIP-1072 competitive assay	18.3[a, f]	5.40[f] (1 h)	31.76[c, f] 135[d, f] 0.096[e, f] (1 h)	[38]
WO2017/027870	Johns Hopkins University	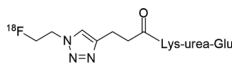	Amplex Red Fluorescence-based assay	12.9[b, g]	47.58[h] (1 h)	164.06[c, h] 432.54[d, h] 2.37[e, h] (1 h)	[39]
WO2017/054907	German Cancer Research Center /Heidelberg University	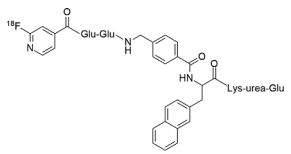	[^{68}Ga]Ga-[Glu-urea-Lys(Ahx)]$_2$-HBED-CC competitive assay	5[a, g]	8.0[g] (1 h)	-	[40]
WO2017/116994	Five Eleven Pharma	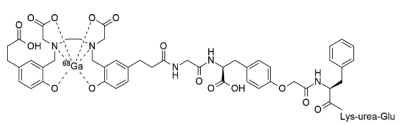	[^{125}I]MIP-1095 competitive binding assay	11.6[a, g]	11.26[g] (1 h)	24.47[c, g] 33.12[d, g] 0.07[e, g] (1 h)	[41]
WO2017/117687	British Columbia Cancer Agency Branch /University of British Columbia	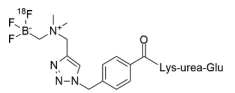	-	-	7.56[g] (2 h)	38.9[c, g] 67.7[d, g] 0.14[e, g] (2 h)	[42]
WO2017/220488	Dextech Medical AB	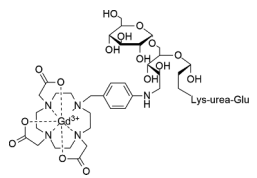	-	-	-	-	[43]
WO2018/005625	Cornell University	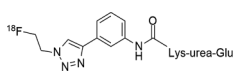	[^{99m}Tc]Tc-MIP-1427 competitive assay	7.0[a, g]	14.30[g] (2 h)	> 10[c, g] > 10[d, g] 0.23[e, g] (2 h)	[44]

(*Continued*)

Table 1. (Continued).

PCT Number	Applicant	Representative compound	assay	IC_{50}(nM)[a] K_i(nM)[b]	Tumor uptake (%ID/g)	Tumor/Blood ratio[c] Tumor/Muscle ratio[d] Tumor/Kidney ratio[e]	Reference
WO2018/102372	Memorial Sloan Kettering Cancer Center	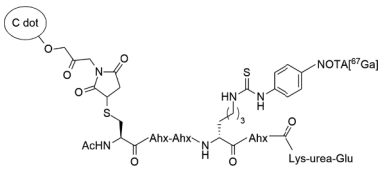	(^{125}I- iPSMA and ^{125}I-(Tyr^4)-bombesin) competitive assay	~7.5[a, g]	~3.5[g] (24 h)	<1[c, g] <5[d, g] <2[e, g] (24 h)	[47]
WO2018/215627	ITM Isotope Technologies Munich AG	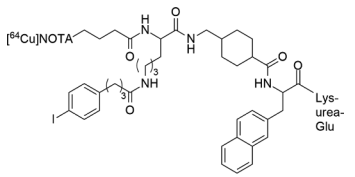	-	-	25.9 %IA/g[h] (1 h) 97.1 %IA/g[h] (24 h)	31.3[c, h] 200[d, h] 2.68[e, h] (24 h)	[48]
WO2018/236115	Futurechem	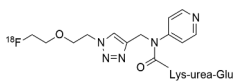	[^{125}I]MIP-1095 competitive assay	5.08[a, f]	-	30.30[c, h] 20.11[d, h] (1 h)	[49]
WO2019/175405	University of Cologne	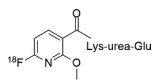	-	-	2.03 %ID/10^5 cells[g] (2 h)	-	[50]
WO2019/190266	Futurechem	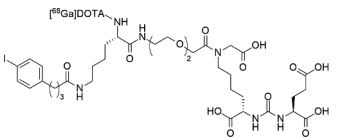	[^{125}I]MIP-1095 competitive assay	11.00[a, f] 3.00[b, f]	7.90[h] (1 h)	2.51[d, h] 0.58[e, h] (1 h)	[52]
WO2020/065045	Heidelberg University /German Cancer Research Center	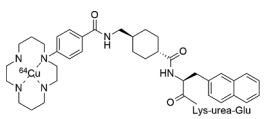	[^{68}Ga]Ga-PSMA-HBED-CC competitive assay	1.60[b, i]	32[i] (4 h)	32[c, i] 32[d, i] 2.46[e, i] (4 h)	[53]

(*Continued*)

Table 1. (Continued).

PCT Number	Applicant	Representative compound	assay	IC_{50}(nM)[a] K_i(nM)[b]	Tumor uptake (%ID/g)	Tumor/Blood ratio[c] Tumor/Muscle ratio[d] Tumor/Kidney ratio[e]	Reference
WO2017/222362	National Institute for Nuclear Research	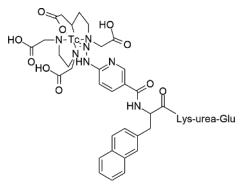	-	2.9[a, g]	8.7[g] (N/A)	-	[54]
WO2017/070482	Johns Hopkins University /Duke University	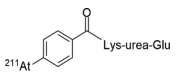	-	-	20.7[h] (2 h)	16.43[c, h] 25.56[d, h] 0.34[e, h] (2 h)	[55]
WO2019/157037	Johns Hopkins University /Duke University	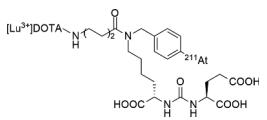	-	-	30.6[h] (1 h)	38.2[c, h] 0.34[e, h] (1 h)	[56]
WO2017/223357	Cornell University	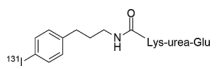	[^{99m}Tc]Tc-MIP-1427 competitive assay	4[a, g]	9.37[g] (24 h)	0.44[c, g] 0.24[e, g] (24 h)	[57]
WO2018/233798	ITM Isotope Technologies Munich AG	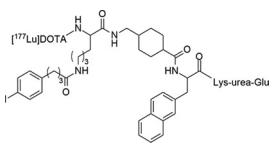	-	-	108[h] (24 h)	77.6[c, h] 514.3[d, h] 10.4[e, h] (24 h)	[58]
WO2019/075583	British Columbia Cancer Agency Branch /University of British Columbia	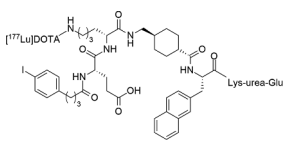	[^{18}F]DCFPyL competitive assay	0.04[b, g]	55.9[g] (24 h)	26.7[c, g] 142[d, g] 0.45[e, g] (24 h)	[59]

(*Continued*)

Table 1. (Continued).

PCT Number	Applicant	Representative compound	assay	IC_{50}(nM)[a] K_i(nM)[b]	Tumor uptake (%ID/g)	Tumor/Blood ratio[c] Tumor/Muscle ratio[d] Tumor/Kidney ratio[e]	Reference
WO2019/115684	Sciencons AS	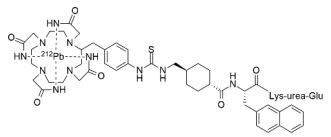	-	-	15.87[g] (2 h)	29.4[c, g] 72.1[d, g] 0.62[e, g] (2 h)	[60]
WO2019/115547	Technical University of Munich	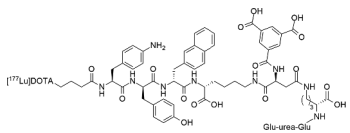	([^{125}I]I-BA)KuE competitive assay	4.0[a, g]	7.70[g] (24 h)	1925.0[c, g] 1100.0[d, g] 1.5[e, g] (24 h)	[61]
WO2019/165200	US Health	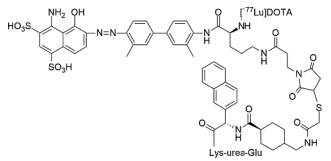	-	7.2[a, h]	~52 (N/A)	~1.67[e]	[62]
WO2019/177499	National Institute for Nuclear Research	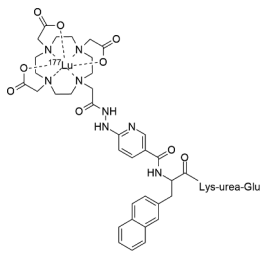	[^{177}Lu]Lu-DOTA-HYNIC-iPSMA Cell-based assay	K_d = 6.33 nM[g]	9.74[g] (N/A)	-	[63]
WO2018/232280	Johns Hopkins University	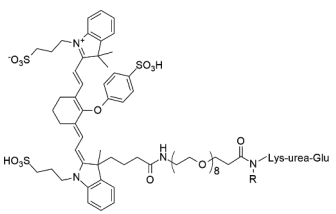	Amplex red Fluorescence-based assay	–	-	-	[64]

(*Continued*)

Table 1. (Continued).

PCT Number	Applicant	Representative compound	assay	IC_{50}(nM)[a] K_i(nM)[b]	Tumor uptake (%ID/g)	Tumor/Blood ratio[c] Tumor/Muscle ratio[d] Tumor/Kidney ratio[e]	Reference
WO2017/044584	On Target Laboratories LCC	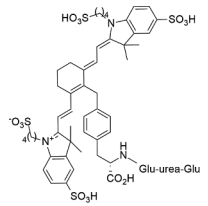	Cell-based flow cytometry assay	K_d = 141.9 nM[f]	-	-	[65]
WO2018/049132	On Target Laboratories LCC	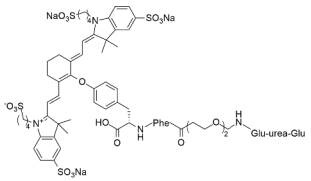	-	-	-	-	[66]
WO2019/183633	Case Western Reserve University	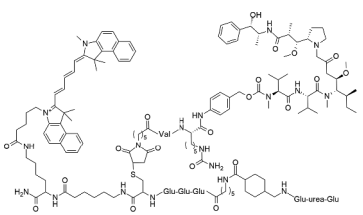	-	Cell viability IC_{50} = 3.56 nM[h]	-	-	[67]
WO2017/205447	Endocyte	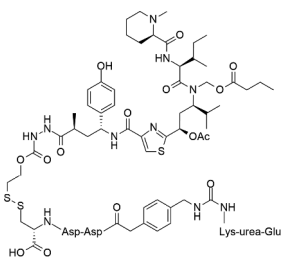	-	-	-	-	[68]

(*Continued*)

Table 1. (Continued).

PCT Number	Applicant	Representative compound	assay	IC_{50}(nM)[a] K_i(nM)[b]	Tumor uptake (%ID/g)	Tumor/Blood ratio[c] Tumor/Muscle ratio[d] Tumor/Kidney ratio[e]	Reference
WO2019/057964	Heidelberg Pharma Research GmbH	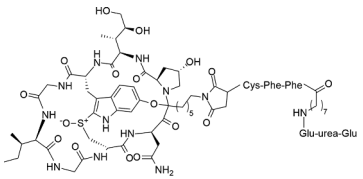	-	Cell viability IC_{50} = 6.11 nM[g]	-	-	[69]
WO2018/098390	Cancer targeted technology LLC	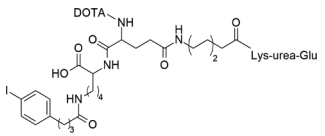	-	-	-	-	[70]
WO2020/028324	Johns Hopkins University /University Health Network	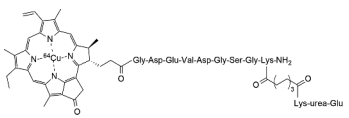	Amplex red Fluorescence-based assay	0.2[b, g]	9.74[h] (17 h)	4.14[c, h] 9.94[d, h] 0.43[e, h] (17 h)	[72]
WO2020/080842	Korea University	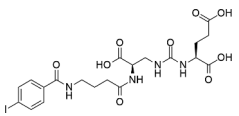	Amplex red Fluorescence-based assay	3.97[a, g]	-	-	[73]

[a]IC_{50}, [b]K_i, [c]Tumor/Blood ratio, [d]Tumor/Muscle ratio, [e]Tumor/Kidney ratio, [f]PSMA+ 22Rv1, [g]PSMA+ LNCaP, [h]PSMA+ PC3 PIP, [i]PSMA+ LNCaP (C4-2) *K_d : Dissociation constant, **K_i : Inhibition constant, ***IC_{50} : Half maximal inhibitory concentration, ****EC_{50}: Half maximal effective concentration

uptake [79]. Monosodium glutamate (MSG) and mannitol were also found to reduce uptake into the kidney and salivary glands [80,81]. For structural modifications of PSMA-targeted agents, the linker region can be utilized to reduce nephrotoxicity. [^{68}Ga]-HTK01167 with 3,3-diphenylalanine moiety as a linker, was reported to present lower kidney uptake than its analogs, which have 2-naphthyl-L-alanine or 2-indanyglycine moiety [82].

It is expected that at least one PET imaging probe in clinical trials, such as [^{18}F]DCFPyL, [^{68}Ga]Ga-PSMA-11, and [^{18}F]PSMA-1007, is likely to be approved and marketed for the diagnosis of metastatic PCa in the near future [30,32,83–85]. ProstaScint, an [^{111}In]-labeled murine monoclonal antibody, has demonstrated poor pharmacokinetic properties and can recognize only the intracellular epitopes of PSMA, limiting its clinical use [86,87]. Therefore, PET imaging of small molecules targeting PSMA is expected to quickly replace ProstaScint in the clinic.

For therapeutic agents targeting PSMA, internalization and recycling of PSMA should be considered for maximum therapeutic effect [88,89]. PSMA-targeted therapeutics must possess a strong binding affinity for PSMA at nanomolar concentrations, be internalized to the cytosol when bound to PSMA, and be retained to some extent in PSMA-expressing cells [11]. The hydrophobic characteristic of PSMA-targeted agents can increase internalization and prolong the circulatory half-life. Therefore, a hydrophobic linker (e.g., 2-naphthyl-L-alanine, 4-iodophenylalkyl group) to interact with the tunnel region [46,90] or the arene-binding site [27,28] can enhance the therapeutic effect of PSMA-targeted agents labeled with α- or β-emitting nuclides. However, it can also affect high uptake into the kidneys and salivary glands, which is undoubtedly overcome.

More recently, PSMA has been used as a carrier for the targeted delivery of cytotoxic agents for metastatic PCa. Conjugates of the PSMA-binding motif (Lys-urea-Glu or Glu-urea-Glu) with cytotoxic agents (e.g., doxorubicin, tubulysin, and amatoxin) have been used to eradicate PSMA-expressing tumor cells [69,91,92]. Internalization, localization, and retention of cytotoxic agents in the cytosol for a sufficient time are key factors for the success of this strategy. In addition, pharmacokinetic studies of conjugates and analyses of degradation processes need to be performed to minimize the potential toxicity of PSMA-expressing organs such as the kidneys and salivary glands. To deliver cytotoxic agents to PSMA-expressing cells with minimal off-target effects in normal tissues, simultaneous targeting of PSMA with another protein (e.g., integrin-$\alpha_v\beta_3$, hepsin, GRPr, etc.) may result in a wide therapeutic index window [93–95]. In addition, co-injection of PSMA-targeted cytotoxic agents with amino acids (penta-L-glutamic acid, MSG), folic poly-L-glutamate, or 2-PMPA can reduce the accumulation of cytotoxic agents in the kidneys [96–98].

It is difficult to provide criteria for optimal PSMA-targeted agents in terms of chemical structure and applied radionuclides. For PSMA inhibitors without a linker moiety, utilization of the S1 accessory pocket of PMSA is recommended to maximize cation-π interaction [16]. In contrast, PSMA inhibitors with a linker moiety need to take advantage of the tunnel region and the arene-binding site. For example, compounds (e.g., PSMA-1007 and PSMA-617) with 2-naphthyl-L-alanine as a linker demonstrated strong PSMA-binding affinity and maximum interaction with the hydrophobic cavity in the tunnel region. In the PSMA crystal complex structure with PSMA-1007 (PDB ID: 5O5T), 2-naphthyl-L-alanine moiety interacts with the lipophilic cavity consisting of Gly548, Tyr552, Tyr549, and Tyr700 in the tunnel next to the S1 accessory pocket (see supplementary material). When developing PSMA-targeted imaging probes by conjugating with bulky prosthetic groups, introduction of a linker that interacts with both the lipophilic cavity of the tunnel region or the arene-binding site will result in high PSMA-binding affinity and tumor uptake. However, for PSMA-targeted therapeutics, the linker structure needs to be optimized to minimize off-target effects. In addition, the physical half-life of applied radionuclides must also be considered. It was observed that therapeutic effect depends on the particle type and physical half-life of the radioisotope [60,99]. It remains controversial which radioisotope is most appropriate for the success of PCa therapy. Further research is needed to identify the optimal linker and the most efficient radioisotope.

Overall, PSMA has potential for the early diagnosis and treatment of patients with metastatic PCa. PET imaging probes targeting PSMA may soon be approved and marketed for clinical use. For therapeutic PSMA agents based on radionuclides or chemotherapy, several important issues including pharmacokinetics, internalization, cellular localization, and nephrotoxicity need to be comprehensively studied.

Funding

This paper was supported by the National Research Foundation of Korea (2019R1A6A1A03031807 and 2020R1A2C2005919)

Declaration of interest

The authors have no relevant affiliations or financial involvement with any organization or entity with a financial interest in or financial conflict with the subject matter or materials discussed in the manuscript. This includes employment, consultancies, honoraria, stock ownership or options, expert testimony, grants or patents received or pending, or royalties.

Reviewer disclosures

Peer reviewers on this manuscript have no relevant financial or other relationships to disclose.

ORCID

Hyunsoo Ha http://orcid.org/0000-0002-9438-1179
Hongmok Kwon http://orcid.org/0000-0001-6858-2674
Taehyeong Lim http://orcid.org/0000-0001-9406-6577
Jaebong Jang http://orcid.org/0000-0002-7962-3395

Song-Kyu Park http://orcid.org/0000-0002-2858-2300
Youngjoo Byun http://orcid.org/0000-0002-0297-7734

References

Papers of special note have been highlighted as either of interest (•) or of considerable interest (••) to readers.

1. Siegel RL, Miller KD, Jemal A. Cancer statistics, 2020. CA Cancer J Clin. 2020;70(1):p. 7–30.
2. *National Cancer Institute*. Available from:https://seer.cancer.gov/statfacts/html/prost.html
3. Bubendorf L, Schopfer A, Wagner U, et al. Metastatic patterns of prostate cancer: an autopsy study of 1,589 patients. Hum Pathol. 2000;31(5):p. 578–583.
4. Partin AW, Kattan M, Subong EN, et al. Combination of prostate-specific antigen, clinical stage, and gleason score to predict pathological stage of localized prostate cancer. A multi-institutional update. JAMA. 1997;277(18):p. 1445–1451.
5. Herschman JD, Smith DS, Catalona WJ. Effect of ejaculation on serum total and free prostate-specific antigen concentrations. Urology. 1997;50(2):p. 239–243.
6. Nadler RB, Humphrey PA, Smith DS, et al. Effect of inflammation and benign prostatic hyperplasia on elevated serum prostate specific antigen levels. J Urol. 1995;154(2):p. 407–413.
7. Mistry K, Cable G. Meta-analysis of prostate-specific antigen and digital rectal examination as screening tests for prostate carcinoma. J Am Board Fam Pract. 2003;16(2):p. 95–101.
8. Carter RE, Feldman AR, Coyle JT. Prostate-specific membrane antigen is a hydrolase with substrate and pharmacologic characteristics of a neuropeptidase. Proc Natl Acad Sci U S A. 1996;93(2):p. 749–753.
9. Silver DA, Pellicer I, Fair WR, et al. Prostate-specific membrane antigen expression in normal and malignant human tissues. Clin Cancer Res. 1997;3(1):p. 81–85.
10. O'Keefe DS, Bacich DJ, Heston WD. Comparative analysis of prostate-specific membrane antigen (PSMA) *versus* a prostate-specific membrane antigen-like gene. Prostate. 2004;58(2):p. 200–210.
11. Liu H, Rajasekaran AK, Moy P, et al. Constitutive and antibody-induced internalization of prostate-specific membrane antigen. Cancer Res. 1998;58(18):p. 4055–4060.
12. Mesters JR, Barinka C, Li W, et al. Structure of glutamate carboxypeptidase II, a drug target in neuronal damage and prostate cancer. Embo J. 2006;25(6):p. 1375–1384.
13. Ghosh A, Heston WD. Tumor target prostate specific membrane antigen (PSMA) and its regulation in prostate cancer. J Cell Biochem. 2004;91(3):p. 528–539.
14. Kwon H, Lim H, Ha H, et al. Structure-activity relationship studies of prostate-specific membrane antigen (PSMA) inhibitors derived from α-amino acid with (S)- or (R)-configuration at P1′ region. Bioorg Chem. 2020;104:p. 104304.
15. Kwon H, Son SH, Byun Y. Prostate-specific membrane antigen (PSMA)-targeted radionuclide probes for imaging and therapy of prostate cancer. Asian J Org Chem. 2019;8(9):p. 1588–1600.
16. Barinka C, Byun Y, Dusich CL, et al. Interactions between human glutamate carboxypeptidase II and urea-based inhibitors: structural characterization. J Med Chem. 2008;51(24):p. 7737–7743.
17. Kozikowski AP, Nan F, Conti P, et al. Design of remarkably simple, yet potent urea-based inhibitors of glutamate carboxypeptidase II (NAALADase). J Med Chem. 2001;44(3):p. 298–301.
18. Kim K, Kwon H, Barinka C, et al. Novel β- and γ-amino acid-derived inhibitors of prostate-specific membrane antigen. J Med Chem. 2020;63(6):p. 3261–3273.
19. Duan X, Liu F, Kwon H, et al. (*S*)-3-(Carboxyformamido)-2-(3-(carboxymethyl)ureido)propanoic acid as a novel psma targeting scaffold for prostate cancer imaging. J Med Chem. 2020;63(7):p. 3563–3576.
20. Kelly J, Amor-Coarasa A, Nikolopoulou A, et al. Synthesis and preclinical evaluation of a new class of high-affinity ^{18}F-labeled PSMA ligands for detection of prostate cancer by PET imaging. Eur J Nucl Med Mol Imaging. 2017;44(4):p. 647–661.
21. Barinka C, Novakova Z, Hin N, et al. Structural and computational basis for potent inhibition of glutamate carboxypeptidase II by carbamate-based inhibitors. Bioorg Med Chem. 2019;27(2):p. 255–264.
22. Yang X, Mease RC, Pullambhatla M, et al. [^{18}F] Fluorobenzoyllysinepentanedioic acid carbamates: new scaffolds for positron emission tomography (pet) imaging of prostate-specific membrane antigen (PSMA). J Med Chem. 2016;59(1):p. 206–218.
23. Jackson PF, Cole DC, Slusher BS, et al. Design, synthesis, and biological activity of a potent inhibitor of the neuropeptidase N-acetylated alpha-linked acidic dipeptidase. J Med Chem. 1996;39(2):p. 619–622.
24. Jackson PF, Tays KL, Maclin KM, et al. Design and pharmacological activity of phosphinic acid based NAALADase inhibitors. J Med Chem. 2001;44(24):p. 4170–4175.
25. Majer P, Jackson PF, Delahanty G, et al. Synthesis and biological evaluation of thiol-based inhibitors of glutamate carboxypeptidase II: discovery of an orally active GCP II inhibitor. J Med Chem. 2003;46(10):p. 1989–1996.
26. Stoermer D, Vitharana D, Hin N, et al. Design, synthesis, and pharmacological evaluation of glutamate carboxypeptidase II (GCPII) inhibitors based on thioalkylbenzoic acid scaffolds. J Med Chem. 2012;55(12):p. 5922–5932.
27. Zhang AX, Murelli RP, Barinka C, et al. A remote arene-binding site on prostate specific membrane antigen revealed by antibody-recruiting small molecules. J Am Chem Soc. 2010;132(36):p. 12711–12716.
28. Cardinale J, Roscher M, Schafer M, et al. Development of PSMA-1007-related series of ^{18}F-labeled glu-ureido-type PSMA inhibitors. J Med Chem. 2020;63(19):p. 10897–10907.
29. Cardinale J, Schafer M, Benesova M, et al. Preclinical evaluation of ^{18}F-PSMA-1007, a new prostate-specific membrane antigen ligand for prostate cancer imaging. J Nucl Med. 2017;58(3):p. 425–431.
30. Calais J, Czernin J, Fendler WP, et al., Randomized prospective phase III trial of ^{68}Ga-PSMA-11 PET/CT molecular imaging for prostate cancer salvage radiotherapy planning [PSMA-SRT]. BMC Cancer. 19(18): 1–11. 2019.

•• **A comprehensive paper describing a Phase III trial of PET imaging with [^{68}Ga]Ga-PSMA-11 that was approved by the US FDA in December 2020 during the review process for this paper.**

31. Rahbar K, Ahmadzadehfar H, Kratochwil C, et al. German multicenter study investigating ^{177}Lu-PSMA-617 radioligand therapy in advanced prostate cancer patients. J Nucl Med. 2017;58(1):p. 85–90.
32. Giesel FL, Knorr K, Spohn F, et al. Detection efficacy of ^{18}F-PSMA-1007 PET/CT in 251 patients with biochemical recurrence of prostate cancer after radical prostatectomy. J Nucl Med. 2019;60(3):p. 362–368.
33. Gorin MA, Rowe SP, Patel HD, et al. Prostate specific membrane antigen targeted ^{18}F-DCFPyL positron emission tomography/computerized tomography for the preoperative staging of high risk prostate cancer: results of a prospective, phase ii, single center study. J Urol. 2018;199(1):p. 126–132.
34. Hofman MS, Violet J, Hicks RJ, et al. [^{177}Lu]-PSMA-617 radionuclide treatment in patients with metastatic castration-resistant prostate cancer (LuPSMA trial): a single-centre, single-arm, phase 2 study. Lancet Oncol. 2018;19(6):p. 825–833.
35. Gorges TM, Riethdorf S, von Ahsen O, et al. Heterogeneous PSMA expression on circulating tumor cells: a potential basis for stratification and monitoring of PSMA-directed therapies in prostate cancer. Oncotarget. 2016;7(23):p. 34930–34941.
36. Kiess AP, Minn I, Chen Y, et al. Auger radiopharmaceutical therapy targeting prostate-specific membrane antigen. J Nucl Med. 2015;56(9):p. 1401–1407.
37. Taylor RM, Severns V, Brown DC, et al. Prostate cancer targeting motifs: expression of alphanu beta3, neurotensin receptor 1, prostate specific membrane antigen, and prostate stem cell

antigen in human prostate cancer cell lines and xenografts. Prostate. 2012;72(5):p. 523–532.
38. Jeong JM, Moon S-H, Lee Y-S, Peptide thiourea derivative, radioisotope labeled compound containing same, And Pharmaceutical Composition Containing Same As Active Ingredient For Treating or Diagnosing Prostate Cancer. WO2017082620A1, 2017.
39. Pomper MG, Chen Y, Yang X, et al. Triazole conjugated ureas, thioureas, carbamates, and "reversed" carbamates for psma-targeted imaging agents and uses thereof. WO2017027870A1., 2017.
40. Cardinale J, Schafer M, Kopka K, et al. ^{18}F-tagged inhibitors of prostate specific membrane antigen (PSMA) and their use as imaging agents for prostate cancer. WO2017054907A1, 2017.
• **A patent that discusses PET imaging clinical trials using ^{18}F-labeled PSMA-targeted agents**
41. Kung HF, Ploessl K, Choi SR, et al. Urea-based prostate specific membrane antigen (PSMA) inhibitors for imaging and therapy. WO2017116994A1, 2017.
42. Benard F, Lin K, Perrin D, et al. $^{18/19}$F-labelled compounds which target the prostate specific membrane antigen. WO2017117687A1, 2017.
43. Holmberg AR, Nisson S, Modified dextran conjugates comprising a lysine-urea-glutamate pharmacophore. WO2017220488A1, 2017.
44. Babich JW, Kelly JM, Amor-Coarasa A, et al. ^{18}F-labeled triazole containing psma inhibitors. WO2018005625A1, 2018.
45. Eder M, Schafer M, Bauder-Wust U, et al. ^{68}Ga-complex lipophilicity and the targeting property of a urea-based PSMA inhibitor for PET imaging. Bioconjug Chem. 2012;23(4):p. 688–697.
46. Benesova M, Bauder-Wust U, Schafer M, et al. Linker modification strategies to control the prostate-specific membrane antigen (PSMA)-targeting and pharmacokinetic properties of DOTA-conjugated PSMA inhibitors. J Med Chem. 2016;59(5):p. 1761–1775.
47. Bradbury MS, Quinn TP, Yoo B, et al. Inhibitor-functionalized ultrasmall nanoparticles and methods thereof. WO2018102372A1, 2018.
•• **Simultaneous targeting of PSMA and gastrin releasing peptide receptor using heterobivalent ligands.**
48. Benesova M, Muller C, Umbricht C, et al. Novel PSMA-binding agents and uses thereof. WO2018215627A1, 2018.
49. Chi DY, Lee BS, Chu SY, et al. ^{18}F-labelled compound for prostate cancer diagnosis, and Use Thereof. WO2018236115A1, 2018.
50. Neumaier B, Zlatopolskiy B, Krapf P, et al. 2-alkoxy-6-[^{18}F]fluoronicotinoyl substituted lys-C(O)-glu derivatives as efficient probes for imaging of psma expressing tissues. WO2019175405A1, 2019.
51. Dietlein F, Hohberg M, Kobe C, et al. An [^{18}]F-labeled PSMA ligand for PET/CT of prostate cancer: first-in-humans observational study and clinical experience with [^{18}]F-JK-PSMA-7 during the first year of application. J Nucl Med. 2020;61(2):p. 202–209.\
52. Chi DY, Lee BS, Chu SY, et al. PSMA-targeted radiopharmaceutical for diagnosing and treating prostate cancer. WO2019190266A1, 2019.
53. Haberkorn U, Dos Santos JC, Mier W, et al. Labeled inhibitors of prostate specific membrane antigen (PSMA), their use as imaging agents and pharmaceutical agents for the treatment of psma-expressing cancers. WO2020065045A1, 2020.
54. Ferro Flores G, Ocampo Garcia BE, Luna Gutierrez MA, et al. ^{99m}Tc-EDDA/HYNIC-iPSMA as a radiopharmaceutical for detecting the overexpression of prostate-specific membrane antigen. WO2017222362A1, 2017.
55. Pomper MG, Mease R, Chen Y, et al. PSMA targeted radiohalogenated ureas for cancer radiotherapy. WO2017070482A2, 2017.
56. Pomper MG, Mease RC, Kumar V, et al. PSMA targeted radiohalogenated urea-polyaminocarboxylates for cancer radiotherapy. WO2019157037A1, 2019.
57. Babich JW, Kelly JM, Amor-Coarasa A, et al. Double targeted constructs to affect tumor kill. WO2017223357A1, 2017.
58. Benesova M, Muller C, Umbricht C, et al. Novel PSMA-binding agents and uses thereof. WO2018233798A1, 2018.
59. Lin K-S, Benard F, Kuo H-T, et al. Novel radiometal-binding compounds for diagnosis or treatment of prostate specific membrane antigen-expressing cancer. WO2019075583A1, 2019.
60. Larsen RH, Complex comprising A PSMA-targeting compound linked to a lead or thorium radionuclide. WO2019115684A1, 2019.
•• **Successful application of ^{212}Pb-labeled PSMA-targeted therapeutics by generating α-particle radiation *in situ*.**
61. Wester H-J, Schmidt A, Parzinger M, PSMA ligands for imaging and endoradiotherapy. WO2019115547A1, 2019.
62. Chen X, Weiss OJ, Chemical conjugates of evans blue derivatives and their use as radiotherapy and imaging agents for targeting prostate cancer. WO2019165200A1, 2019.
63. Ferro Flores G, Ocampo Garcia BE, Luna Gutierres MA, et al. ^{177}Lu-DOTA-HYNIC-iPSMA as a therapeutic radiopharmaceutical targeting prostate-specific membrane antigen. WO2019177449A1, 2019.
•• **Successful combination of PET imaging with gallium-68 and tumor treatment with lutetium–177.**
64. Pomper MG, Mease RC, Chen Y, et al. PSMA targeted fluorescent agents for image guided surgery. WO2018232280A1, 2018.
65. Kularatne SA, Low P, Gagare P, et al. PSMA-targeted NIR dyes and their uses. WO2017044584A1, 2017.
66. Kularatne SA, Gagare P, PSMA-targeted nir dyes and their uses. WO2018049132A1, 2018.
67. Basilion JP, Wang X, Walker N, PSMA targeted conjugate compounds and uses thereof. WO2019183633A1, 2019.
68. Leamon C, Nguyen B, Methods of treating cancer with a psma ligand-tubulysin compound. WO2017205447A1, 2017.
•• **Diagnosis with technetium-99m, followed by tumor treatment with PSMA-tubulysin conjugate.**
69. Gallo F, Korsak B, Mueller C, et al. PSMA-targeting amantin conjugates. WO2019057964A1, 2019.
70. Berkman C, Choy C, Albumin-binding PSMA inhibitors. WO2018098390A1, 2018.
71. Kelly JM, Amor-Coarasa A, Nikolopoulou A, et al. Dual-target binding ligands with modulated pharmacokinetics for endoradiotherapy of prostate cancer. J Nucl Med. 2017;58(9):p. 1442–1449.
72. Pomper MG, Mease RC, Chen Y, et al. Long-circulating PSMA-targeted phototheranostic agent. WO2020028324A1, 2020.
• **Therapeutic potential of photo-theranostic agents targeting PSMA.**
73. Byun Y, Son S-H, Kim K, et al. Prostate-specific membrane antigen inhibitor for diagnosing and treating prostate cancer, and pharmaceutical composition for diagnosing and treating prostate cancer containing same. WO2020080842A1, 2020.
74. Maurer T, Eiver M, Schwaiger M, et al. Current use of PSMA-PET in prostate cancer management. Nat Rev Urol. 2016;13(4):p. 226–235.
75. Perera M, Papa N, Christidis D, et al. Sensitivity, specificity, and predictors of positive ^{68}Ga-prostate-specific membrane antigen positron emission tomography in advanced prostate cancer: a systematic review and meta-analysis. Eur Urol. 2016;70(6):p. 926–937.
76. Afshar-Oromieh A, Babich JW, Kratochwil C, et al. The rise of PSMA ligands for diagnosis and therapy of prostate cancer. J Nucl Med. 2016;57(Suppl 3):p. 79S–89S.
77. de Galiza Barbosa F, Queiroz MA, Nunes RF, et al. Nonprostatic diseases on PSMA PET imaging: a spectrum of benign and malignant findings. Cancer Imaging. 2020;20(1):p. 23.
78. Saffar H, Noohi M, Tavangar SM, et al. Expression of prostate-specific membrane antigen (PSMA) in brain glioma and its correlation with tumor grade. Iran J Pathol. 2018;13(1):p. 45–53.
79. Kratochwil C, Giesel FL, Leotta K, et al. PMPA for nephroprotection in PSMA-targeted radionuclide therapy of prostate cancer. J Nucl Med. 2015;56(2):p. 293–298.
80. Matteucci F, Mezzenga E, Caroli P, et al. Reduction of ^{68}Ga-PSMA renal uptake with mannitol infusion: preliminary results. Eur J Nucl Med Mol Imaging. 2017;44(13):p. 2189–2194.

81. Rousseau E, Lau J, Kuo HT et al. Monosodium glutamate reduces ^{68}Ga-PSMA-11 uptake in salivary glands and kidneys in a preclinical prostate cancer model. J Nucl Med. 2018;59(12):p. 1865–1868.
82. Kuo HT, Pan J, Zhang Z, et al. Effects of linker modification on tumor-to-kidney contrast of ^{68}Ga-labeled PSMA-targeted imaging probes. Mol Pharm. 2018;15(8):p. 3502–3511.
83. Szabo Z, Mena E, Rowe SP, et al. Initial evaluation of [^{18}F]DCFPyL for prostate-specific membrane antigen (PSMA)-targeted PET imaging of prostate cancer. Mol Imaging Biol. 2015;17(4):p. 565–574.
84. Morris MJ, Carroll PR, Saperstein L, et al. Impact of PSMA-targeted imaging with ^{18}F-DCFPyL-PET/CT on clinical management of patients (pts) with biochemically recurrent (BCR) prostate cancer (PCa): results from a phase III, prospective, multicenter study (CONDOR). J Clin Oncol. 2020;38(15 suppl):p. 5501.
85. Wang J, Zang J, Wang H, et al. Pretherapeutic ^{68}Ga-PSMA-617 PET may indicate the dosimetry of ^{177}Lu-PSMA-617 and ^{177}Lu-EB-PSMA-617 in main organs and tumor lesions. Clin Nucl Med. 2019;44(6):p. 431–438.
86. Bander NH. Technology insight: monoclonal antibody imaging of prostate cancer. Nat Clin Pract Urol. 2006;3(4):p. 216–225.
87. Barren RJ 3rd, Holmes EH, Boynton AL, et al. Monoclonal antibody 7E11. C5 staining of viable LNCaP cells. Prostate. 1997;30(1):p. 65–68.
88. Rajasekaran SA, Anilkumar G, Oshima E, et al. A novel cytoplasmic tail MXXXL motif mediates the internalization of prostate-specific membrane antigen. Mol Biol Cell. 2003;14(12):p. 4835–4845.
89. Begum NJ, Glatting G, Wester HJ, et al. The effect of ligand amount, affinity and internalization on PSMA-targeted imaging and therapy: a simulation study using a PBPK model. Sci Rep. 2019;9(1):p. 20041.
90. Wüstemann T, Bauder-Wust U, Schafer M, et al. Design of Internalizing PSMA-specific glu-ureido-based radiotherapeuticals. Theranostics. 2016;6(8):p. 1085–1095.
91. Ivanenkov YA, Machulkin AE, Garnina AS, et al. Synthesis and biological evaluation of doxorubicin-containing conjugate targeting PSMA. Bioorg Med Chem Lett. 2019;29(10):p. 1246–1255.
92. Leamon CP, Reddy JA, Bloomfield A, et al. Prostate-specific membrane antigen-specific antitumor activity of a self-immolative tubulysin conjugate. Bioconjugate Chem. 2019;30(6):p. 1805–1813.
93. Subedi M, Minn I, Chen J, et al. Design, synthesis and biological evaluation of PSMA/hepsin-targeted heterobivalent ligands. Eur J Med Chem. 2016;118(p):208–218.
94. Shallal HM, Minn I, Banerjee SR, et al. Heterobivalent agents targeting PSMA and integrin-$\alpha_v\beta_3$. Bioconjugate Chem. 2014;25(2):p. 393–405.
95. Abouzayed A, Yim CB, Mitran B, et al. Synthesis and preclinical evaluation of radio-iodinated GRPR/PSMA bispecific heterodimers for the theranostics application in prostate cancer. Pharmaceutics. 2019;11(7):p. 358.
96. Pomper MG, Mease RC, Ray S, et al. Competitive prostate-specific membrane antigen (PSMA) binding agents for the reduction of non-target organ uptake of radiolabeled PSMA inhibitors for PSMA positive tumor imaging and radiopharmaceutical therapy. WO2020028323A1, 2020.
97. Sarnelli A, Belli ML, Di Iorio V, et al. Dosimetry of ^{177}Lu-PSMA-617 after mannitol infusion and glutamate tablet administration: preliminary results of EUDRACT/RSO 2016-002732-32 IRST protocol. Molecules. 2019;24:3.
98. Uehara T, Minegishi Y, Kise S, et al. Reduced renal uptake of ^{68}Ga-PSMA-617 by penta-l-glutamic acid co-injection. J Nucl Med. 2018;59 no(1):p. 1279. supplement.
99. Stenberg VY, Juzeniene A, Chen Q, et al. Preparation of the alpha-emitting prostate-specific membrane antigen targeted radioligand [^{212}Pb] Pb-NG001 for prostate cancer. J Labelled Comp Radiopharm. 2020;63(3):p. 129–143.